Environmental
Studies
Revolving
Funds

035

Further Studies on the Assessment of Marine Radars for the Detection of Icebergs

Canada

June 1986

The Environmental Studies Revolving Funds are financed from special levies on the oil and gas industry and administered by the Canada Oil and Gas Lands Administration for the Minister of Energy, Mines and Resources, and by the Northern Affairs Program for the Minister of Indian Affairs and Northern Development.

Environmental Studies Revolving Funds
Report No. 035

June 1986

FURTHER STUDIES ON THE ASSESSMENT OF MARINE RADARS FOR THE DETECTION OF ICEBERGS

Michael J. Harvey
Joseph P. Ryan

Viatec Resource Systems Inc.
#114, 6815 - 8th Street N.E.
Calgary, Alberta
T2E 7H7

Scientific Authority: Dr. S. Haykin

The correct citation for this report is:

Harvey, M.J. and J.P. Ryan. 1986. Further studies on the assessment of marine radars for the detection of icebergs. Environmental Studies Revolving Funds Report No. 035. Ottawa. 82p.

Published under the auspices
of the Environmental Studies
Revolving Funds
ISBN 0920783-34-1

TABLE OF CONTENTS

LIST OF TABLES

LIST OF FIGURES

ABBREVIATIONS

The following is a list of major abbreviations used in this report:

A/D	Analogue to digital
ARPA	Automatic radar plotting aid
BB	Bergy Bit
B & W	B & W Electronik AS Scanner 8000 Radar Display
CFAR	Constant false alarm rate
CP	Clutter Power
DMA	Direct memory access
DR	Dynamic Range
GRW	Growler
HSA	Horizontal sextant angle
LBL	Large blocky
LDD	Large dry dock
LDM	Large dome
LOGSEC	Data-logging software program (sectors)
LPI	Large pinnacle
LTA	Large tabular
LWD	Large wedge
MBL	Medium blocky
MDD	Medium dry dock
MDM	Medium dome
MDS	Minimum detectable signal
MPI	Medium pinnacle
MTA	Medium tabular
MWD	Medium wedge
naut mi	Nautical mile
NRCS	Normalized radar cross-section
PPI	Plan position indicator
PPILOG	Data logging software program (scans)
PRF	Pulse repetition frequency
SAR	Synthetic aperture radar
SBL	Small blocky
S/C	Signal-to-clutter ratio
SDD	Small dry dock
SDM	Small dome
SNR	Signal-to-noise ratio
STC	Sensitivity time control
SWD	Small wedge
SWH	Significant wave height
TR	Transmit-receive
VSA	Vertical sextant angle
VERIFY	Data verification software program
WS	Wind speed

PARAMETERS

The following terms and units of measure are used in the text and in equations.

C	Clutter power (Watts)
c	Speed of light (m/s)
dBM	Decibels below 1 milliwatt (mW)
F	Propagation factor
G	Antenna gain (dB)
h_d	Height of duct (m)
kW	Kilowatt
kt	Knot
L	Radar losses
l	Duct stability
N	Noise power (Watts)
n	Number of pulses per beamwidth
naut mi	Nautical mile
n_{sa}	Sea-air refractivity index
Pd	Probability of detection
Pfa	Probability of false alarm
P_r	Power received (Watts)
P_t	Peak transmitter power (Watts)
R	Range to iceberg (m) (naut mi)
S	Signal power (Watts)
T_{fa}	Time between false alarms
τ	Pulse length (microseconds)
σ	Radar cross-section (m^2)
σ°	Normalized radar cross-section (m^2/m^2)
θ	Beamwidth (deg.)
λ	Radar wave length (m)

ACKNOWLEDGEMENTS

The authors would like to acknowledge the assistance and guidance provided throughout the field trials by Greg Warbanski of Husky/Bow Valley, Dave Pearson formerly of Petro-Canada, Jacques Benoit of Mobil Oil Canada, and Dr. Simon Haykin of McMaster University.

Without the excellent co-ordination of human, material, and financial resources made possible through the efforts of Peter Wood, formerly of the Environmental Studies Revolving Funds, this study would not have been conducted.

Finally, Petro-Canada, Mobil Oil Canada, the Carino Shipping Company, the McGill Weather Radar Observatory, and Mike McNeil of Environmental Studies Revolving Funds provided valuable equipment and support services.

The project team was comprised of Michael Harvey, Joseph Ryan, Dean White, Marlowe House, Andrew Kent, Mata Bishun, and Kathryn Knauff.

SUMMARY

To thoroughly investigate the iceberg detection capability of shipborne marine radar, a field program was carried out aboard the MV Polar Circle in the northern area of the Grand Banks of Newfoundland area during April 1985. The data collected is able to provide information on icebergs in sea clutter, emphasizing small icebergs, and to demonstrate the advantages of signal processing to maximize detection capability. The data have been used to validate a radar model that can predict radar performance under a variety of operational and environmental conditions by modifying the input parameters.

During the data collection program, a high-resolution digital radar-recording system was employed in conjunction with a specially installed Racal-Decca FI 2459 combined (S/X) system which uses antennas that are co-located and synchronized. The antenna height for this system was 15-m. Recording of raw radar video signals was accomplished for icebergs, sea ice, calibrated targets, sea clutter and other targets of opportunity. Because of the mobility of the ship, many data were collected for each target, and a thorough verification of the data was completed.

The raw video signals from each radar were digitized sequentially and were stored on standard nine-track computer tape. The video was digitized at different sampling rates with 8-bit quantitization. A thorough system calibration was completed.

The data set includes 38 measured icebergs of various sizes and types, volumes of sea clutter and other target data collected under a range of environmental conditions with significant wave height ranging from 0-7 m, and wind speeds ranging from 0-35 kt.

Much analysis software was produced to enable quantitative analysis test of selected data points for model verification and to trial signal processing techniques. Four important findings follow.

a) There was excellent agreement between the data of Nathanson (1969) and the field data for X-band sea clutter. S-band sea clutter is more variable, but is generally in agreement.

b) Measurements of radar cross-sections of icebergs indicate that X-band radar cross-sections are up to 10 times larger than those of S-band. These results agree with those of current X-band models.

c) A blip-to-scan analysis has enabled a quantification of the improvement in target detectability when scan-averaging is implemented. It is shown that scan-averaging is a powerful technique in the iceberg environment.

d) Operationally, S-band radar appears superior, but increasing antenna height seems to improve maximum detection ranges in all cases when signal-processing techniques are not used.

RÉSUMÉ

Afin d'examiner à fond la capacité des radars de navires à détecter les icebergs, on a effectué un programme-terrain à bord du vaisseau à moteur Polar Circle dans la région Nord des Grands Bancs de Terre-Neuve en avril 1985. Les données recueillies fournissent des renseignements sur les icebergs parmi les échos de vague, surtout les petits icebergs, et prouvent les avantages du traitement des signaux pour porter au maximum la capacité de détection. Les données ont servi à rendre valable un modèle de radar capable de prédire le rendement du radar dans toute une gamme de conditions fonctionnelles et environnementales en modifiant les paramètres d'entrée.

Au cours du programme de collecte des données, on a utilisé un enregistreur de radar numérique à haute résolution en compagnie d'un radar à bandes X et S Racal Decca FI 2459 d'installation spéciale, muni d'antennes placées au même endroit et synchronisées. La hauteur de l'antenne pour ce système était de 15 m. Les enregistrements d'images radar sans élimination d'échos perturbateurs ont été effectués pour les icebergs, la glace de mer, les cibles étalonnées, les échos de vague et d'autres cibles possibles. À cause de la mobilité du vaisseau, on a recueilli une grande quantité de données pour chaque cible et cela a permis également d'effectuer des références-terrain approfondies.

Les images de radar sans élimination d'échos perturbateurs de chaque radar ont été numérisées séquentiellement et mémorisées sur une bande ordinaire à neuf pistes pour ordinateur. Les images ont été numérisées à divers taux d'échantillonnage avec une quantification de huit bits. Un étalonnage complet du système a été effectué.

L'ensemble de données comprend 38 icebergs de dimensions et de genres variés, des volumes de données portant sur les échos de vague et d'autres cibles recueillies dans tout un éventail de conditions atmosphériques et avec des vagues dont la hauteur variait de 0-7 m, et la vélocité du vent de 0-35 noeuds.

Une grande quantité de programmes d'analyse a été produite afin de permettre l'analyse quantitative d'un nombre choisi de points de données pour la vérification des modèles et l'essai des techniques de traitement des signaux. Quatre importantes conclusions sont résumées ci-dessous :

a) Un accord excellent a existé entre les données de Nathanson(1969) et les données-terrain pour les échos de vague de la bande X. Les échos de vague de la bande S sont plus variables, mais ils sont habituellement en accord.

b) Les mesures de la portée du radar pour la surveillance des icebergs indiquent que la portée du radar à bande X va jusqu'à 10 fois plus loin que celle du radar à bande S. Ces résultats correspondent à ceux des modèles actuels à bande X.

c) Un top d'écho à l'analyse de balayages a permi une quantification de l'amélioration de la détection des cibles lors de la mise en oeuvre d'une moyenne des balayages. Il a été démontré que la moyenne des balayages est une méthode puissante en milieu d'icebergs.

d) Sur le plan du rendement, le radar à bande X semble supérieur, mais la hauteur croissante des antennes semble être le principal facteur pour l'amélioration des portées maximales de détection dans tous les cas où les techniques de traitement des signaux ne sont pas utilisées.

1.0 INTRODUCTION

While efforts to explore for and extract oil from east coast reservoirs continue, so does research to overcome the problems of iceberg management. Surface-based microwave radars are likely to continue to be used as one of the major methods for the detection of ice and icebergs. Commencing in 1984 the Environmental Studies Revolving Funds (ESRF) funded a program entitled "The Assessment of Marine Radars for the Detection of Ice and Icebergs." The aim of the study was to provide a quantitative assessment of the capability to detect icebergs of existing marine radars. To meet that aim, a field program was mounted using the semi-submersible SEDCO-706, which was chosen from a number of options including vessels and even land-based sites. Because of its stability, choice of radars, location, and simplified logistics requirements to support the program, it appeared to be the most feasible option to pursue with the funding available.

The results of this work were reported by Ryan et.al. (1985). Briefly, following selection of a platform, two X-band and the two S-band radar systems on board the SEDCO-706 were instrumented with a digital recording system. Twelve, well-documented, iceberg targets were recorded over the course of the 3 month program. Although a statistical analysis was not possible because of the relatively few data, the calculated iceberg cross-sections confirmed, for the most part, the relationship derived by Budinger (1960). The large number of possible system, operational, and environmental parameters makes it impossible to collect a set of radar data for each different situation. Therefore, a model was produced as part of the study to predict radar performance in most situations. This model was then validated using the data collected in the field. Again good results were achieved. The data illustrated certain environmental effects which affected detectability, such as ducting and subrefraction, and provided valuable information on sea clutter. It was possible to calculate radar cross-sections of icebergs and the ocean in a wide range of sea states.

Unfortunately, few data were obtained for targets in sea clutter. Although the values obtained for normalized radar cross-sections of the ocean agreed in some cases with published data and the model, other cases did not agree. There was not a large enough number of icebergs to correlate their radar cross-sections with their average cross-sectional area with a high degree of confidence.

These limitations to the data did not prevent the field program from meeting its objectives constrained by the limited resources available, but they did point to a need for further work to enable a complete and proper assessment of the detectability of ice and icebergs by conventional, microwave, marine radar.

A number of recommendations resulted from the 1984 field work and subsequent analysis. The major recommendations included:

- that an ongoing program to acquire a data base for radar cross-sections of icebergs on the Grand Banks be conducted;

- that a data collection program to obtain radar data for small ice targets in sea clutter be undertaken;

- that meteorological parameters be collected with which to calculate evaporation duct parameters, which, in turn, would enable the development of a long-term propagation guide for operational use; and

- that data-processing techniques be investigated for enhancing target detectability

These recommendations were accepted by the ESRF and an extension to the study was authorized. To meet the primary aim of the program to quantify iceberg detection capability, a number of objectives were to be emphasized. These included the collection of more data on radar cross-sections of icebergs, data containing small-to-medium icebergs and ice in different environmental conditions, especially those which promote clutter returns, and the investigation of data-processing techniques for improving detection capability. The recommendation concerning the collection of ducting parameters was to be de-emphasized, although verification data required for its prediction were collected as a matter of course during the experiment.

As in the 1984 program, the 1985 extension consisted of phases for a planning and mobilization, field data collection on board the research vessel MV Polar Circle, and data analysis.

During the planning and mobilization phase, the opportunity to improve on last season's activity presented itself. A dedicated radar system was acquired for the program and a new improved higher-resolution radar interface was produced by Viatec. Because a vessel was selected, a much greater variety of situations were encountered as well as a much greater number of icebergs. The Racal-Decca Combined 2459 F/I radar was installed at typical work-boat height to collect data during April. In total, data on 42 icebergs of all sizes, 23 ice targets, and a tremendous amount of sea clutter were collected. In addition, a number of vessels, calibrated targets, and land targets were recorded. Because of its inherent motion, the limitations of using a vessel rather than an exploration platform is acknowledged, but, these effects are a fact of operational life and must be considered. However, they can be minimized, and, in most cases, did not affect the data to a large extent.

With many, high-quality data collected, the analysis phase was expanded in scope from that originally proposed. However, only a sampling of data was analyzed in each of the areas of interest. A statistical analysis, now possible with the many data, was not conducted. Instead, efforts were concentrated upon producing a well-documented data set including data on magnetic tape, accompanying field notes, meteorological records, and iceberg photographs and observations. Duplication of the data set was also completed. This report contains a complete set of verification data and instructions for its use.

To assess detectability of even a limited number of targets, which in this report have been limited to glacial ice targets, extensive analysis software was produced, which enabled the data to be compared with the upgraded radar model also available for this study. This capability enables predictions of detection capability versus sea state and potential improvements to display capability to be presented quantitatively.

2.0 DATA COLLECTION METHODOLOGY

2.1 GENERAL

With a decision to proceed with the field program, the first work to be completed was that of locating an appropriate platform from which to conduct the work. To ensure that a wide variety and large number of ice and icebergs could be recorded, as well as collecting a complementary, rather than supplementary, data set to that collected in 1984, the platform chosen for the 1985 iceberg season was a ship. Once a ship was identified, a charter was signed, the necessary radar equipment was then procured and prepared, and installation and testing of equipment and software commenced. Following testing at sea, the data collection activity began in earnest.

Although in 1984 the ship had not been considered an ideal platform for the first data collection, primarily because of the perception that it would roll and pitch in heavy or even moderate seas, it was considered more attractive in 1985. The presence of a limited data set from the stable platform of SEDCO 706 would enable a comparison with data collected from a ship, with the possibility of compensating for vessel motion, if any, in any subsequent analysis. As it turned out, vessel motion was minimal and did not affect the data set.

The data acquisition plan in detail was submitted for approval by ESRF prior to commencing the installation of on board the ship. It amplifies the rationale for using a ship, rather than a platform and details the ship, the proposed recording system, and proposed recording and verification, methodology.[1]

2.2 THE EQUIPMENT

It is interesting to note the complexity of installing a small data-acquisition system on board a mobile platform.The MV Polar Circle was used for the collection of radar data during April 1985. The radars used were the same as for the 1984 program on board the SEDCO 706 semi-submersible drilling platform mounted on the derrick top. This Racal-Decca F/I 2459 Dual Radar System, one X-band and one S-band, replaced one radar of the MV Polar Circle using a reinforced mounting.

1 Assessment of marine radars for the detection of ice and icebergs (Program extension). Mobilization and Data Acquisition Plan final report submitted to Environmental Studies Revolving Funds by Viatec Resource Systems Inc., February 1985.

Table 2.1.
Specification and physical characteristics of X- and S-band radar systems

Specification	Characteristics	
	X-band	S-band
Frequency (MHz)	9410 ± 30	3050 ± 10
Transmitter peak power, (KW)	18.5	27.0
Pulse length (usec)	1.0, 0.25, 0.05	1.0, 0.25, 0.05
Pulse repetition frequency (PPS)	825, 1650, 3300	825, 1650, 3300
Receiver bandwidth (MHz)	5 and 18	5 and 18
Receiver noise figure (dB)	10.0	3.5
Horizontal beamwidth, 3 dB (Deg)	0.8	2.0
Vertical beamwidth, 3 dB (Deg)	20	30
Antenna gain (dB)	31	26
System losses (dB)	6.0	6.0
Antenna height (m)	15	15
Number of pulses per beamwidth	3.7	9.2
Number of pulses per beamwidth recorded	2.3	5.7

The scanner was located on the mast directly above the wheelhouse. This ideal spot allowed the transceivers to be mounted in the stairwell to the crow's-nest close to the antennas, keeping waveguide loses to a minimum. This location provided easy access, just above the radio room, in all kinds of weather to take readings for calibration and power output. The height of the antennas plus extra mounting structure was 15 m above sea-level.

The radar system with recording configuration is illustrated in Figure 2.1.The radar signals (i.e., video, trigger, and synchro) to the B & W Electronik As Scanner 8000 radar display (B & W) and ARPA display units from the video combiner unit were also connected to the radar interface. The video combiner unit allowed control of pulse length, tuning, and scanner unit. The front-end section of the interface contained signal multiplexing to allow operator control and easier switching between X- and S-band radar signals. The video-to-digital conversion unit was capable of sampling at either 4 MHz or 8 MHz with a 256-level quantization. This digital conversion was performed on the peak radar video signals for a given sampling interval. The three-phase synchro signal was converted to a digital azimuth word and was combined with the radar interface status which comprised the radial header word. For each radial, the header word was transferred to the computer followed by digital video information. About two out of every three radar sweeps were recorded in this manner. Transfer of digital signals was achieved using direct memory access (DMA) on a PDP 11/23+ microcomputer. A Kennedy, nine-track, tape drive was used to store all digital information and control of the microcomputer software was performed from a VT100 computer terminal.

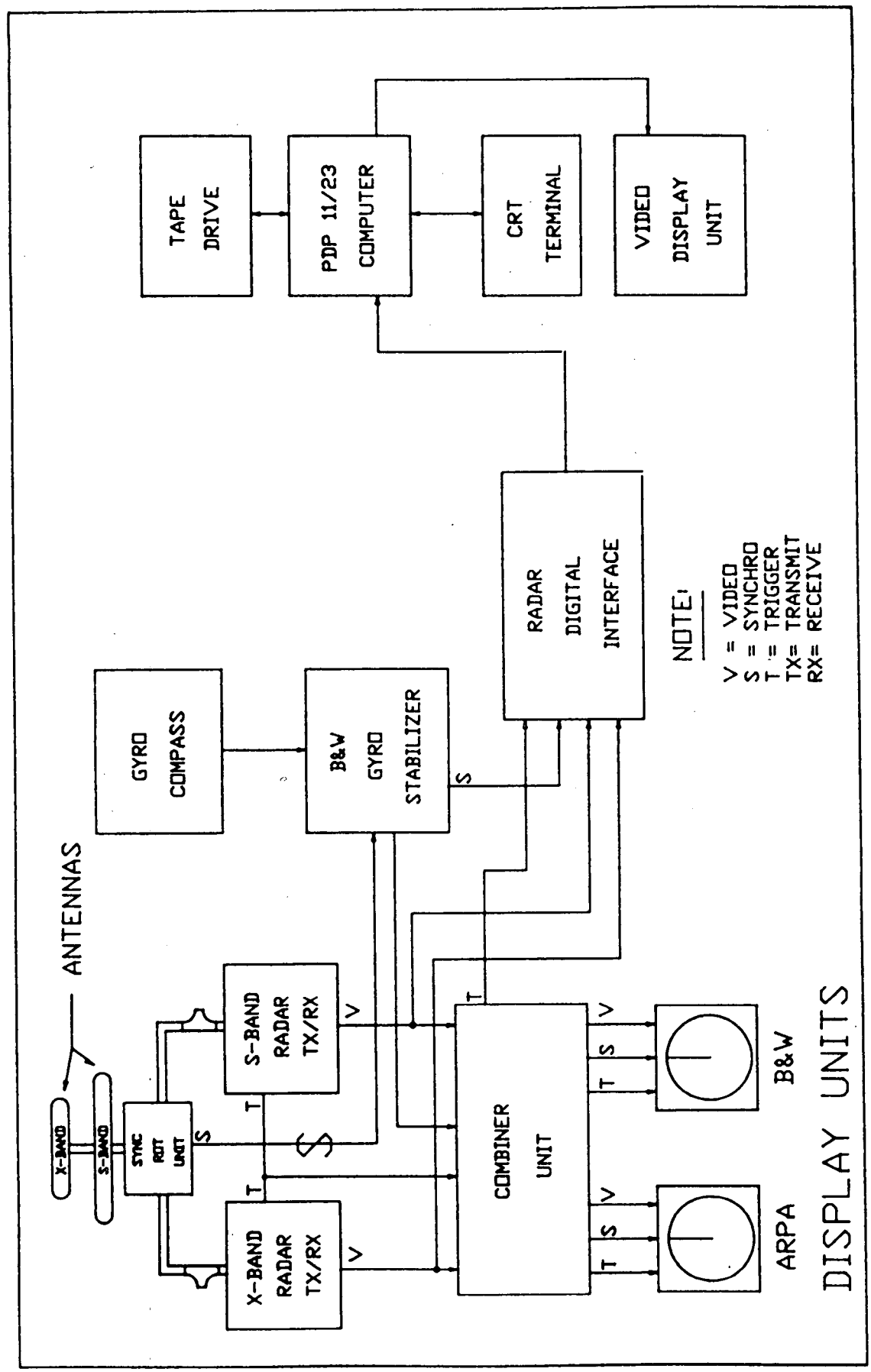

Figure 2.1. Configuration of radar recording system.

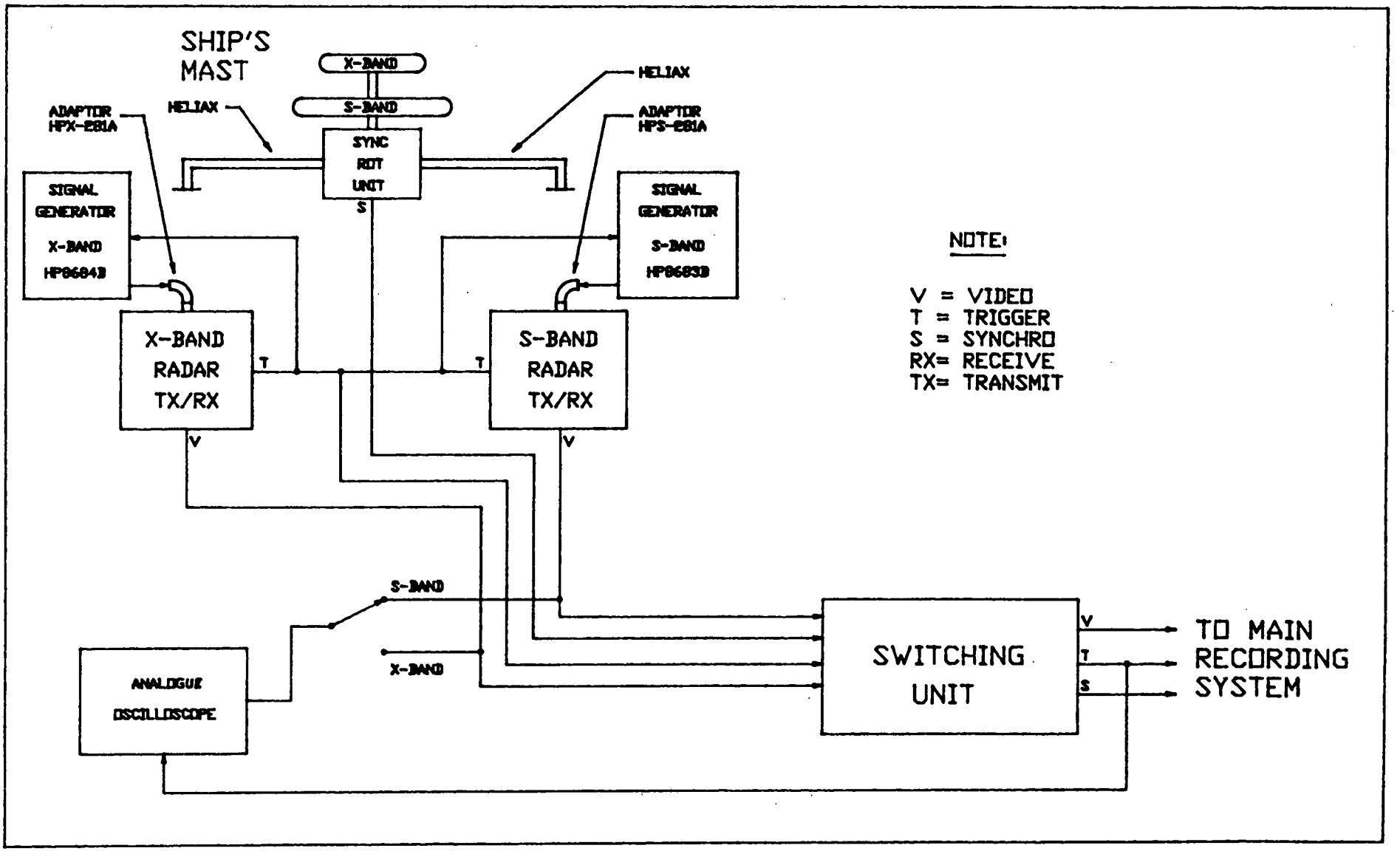

Figure 2.2. Configuration for calibration of receiver units.

Included on the ship's equipment list are the two display units, ARPA and B & W. ARPA, the primary display unit, was used for tracking icebergs and for gathering range and bearing data. These data were used by the operator to input to the computer to initiate the recording sequence. The B & W display unit was used as a back-up display unit that proved useful because it had better sensitivity than the ARPA unit. The main function for the B & W display on board the MV Polar Circle was to stabilize the three-phase synchro lines from the scanner unit. The stabilization (north-up mode) was made possible using data from the ship's fitted gyro-compass.

The ship's remaining radar, mounted on top of the crow's-nest, at an elevation of 21 m also proved useful. With greater antenna height the radar horizon was significantly increased.

2.3 SYSTEM CALIBRATION

The system calibrated in two steps. The first step was to calibrate the analogue circuits which included the X- and S-band receiver units, the combiner unit, line losses, and the analogue portion of the radar digitizer interface Figure 2.2. This portion of the calibration was carried out using HP8683B and HP8684B signal generators that produced microwave frequencies. The microwave signals were injected into the waveguide at the receiver and the resultant analogue voltage was measured at the radar interface with all recording equipment connected and running. For the two receiver units the output voltage was recorded against the input power. The data were recorded in 5-dB steps from the minimum detectable signal (MDS) to saturation and back down again where power was measured in dBm (decibels below 1 milliWatt). The second step required calibration of the analogue-to-digital (A/D) converter circuit. This simple step was achieved using a built-in calibration circuit that placed a voltage on the A/D circuit which was recorded against the resultant digital signal. Combining these two steps resulted in the calibrated data, output voltage (binary) versus input power (dBm).

During the acquisition program, the system was changed several times. After each change the system was recalibrated and the data were recorded. For each calibration the data were plotted. Listed in the caption are the signal type and tape numbers for which each data set is valid. An example is provided as Figure 2.3.

Transmitter power was measured daily and was recorded in the field notes. Figure 2.4 illustrates the method used.

A number of recurring and non-recurring problems were encountered with the equipment. These problems are documented and are retained by Viatec Resource Systems Inc. but do not affect integrity of the data set.

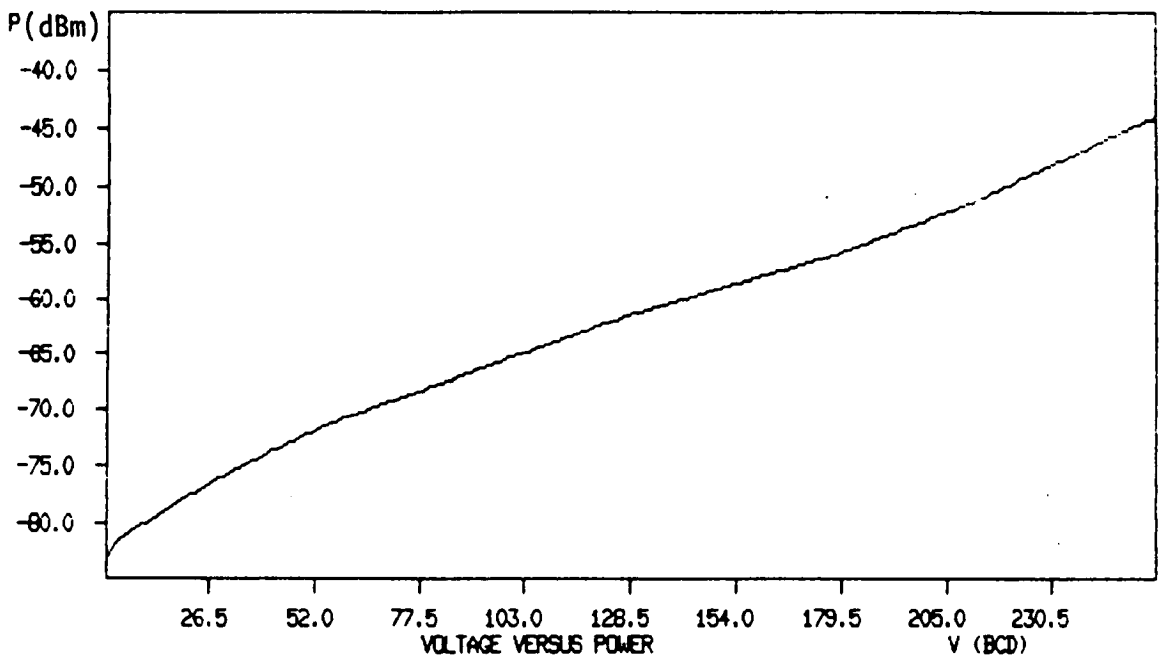

Figure 2.3 Calibration data for X-band, medium pulse with approximately 2 dB attenuation (#58 ≤ Tapes ≤ #62).

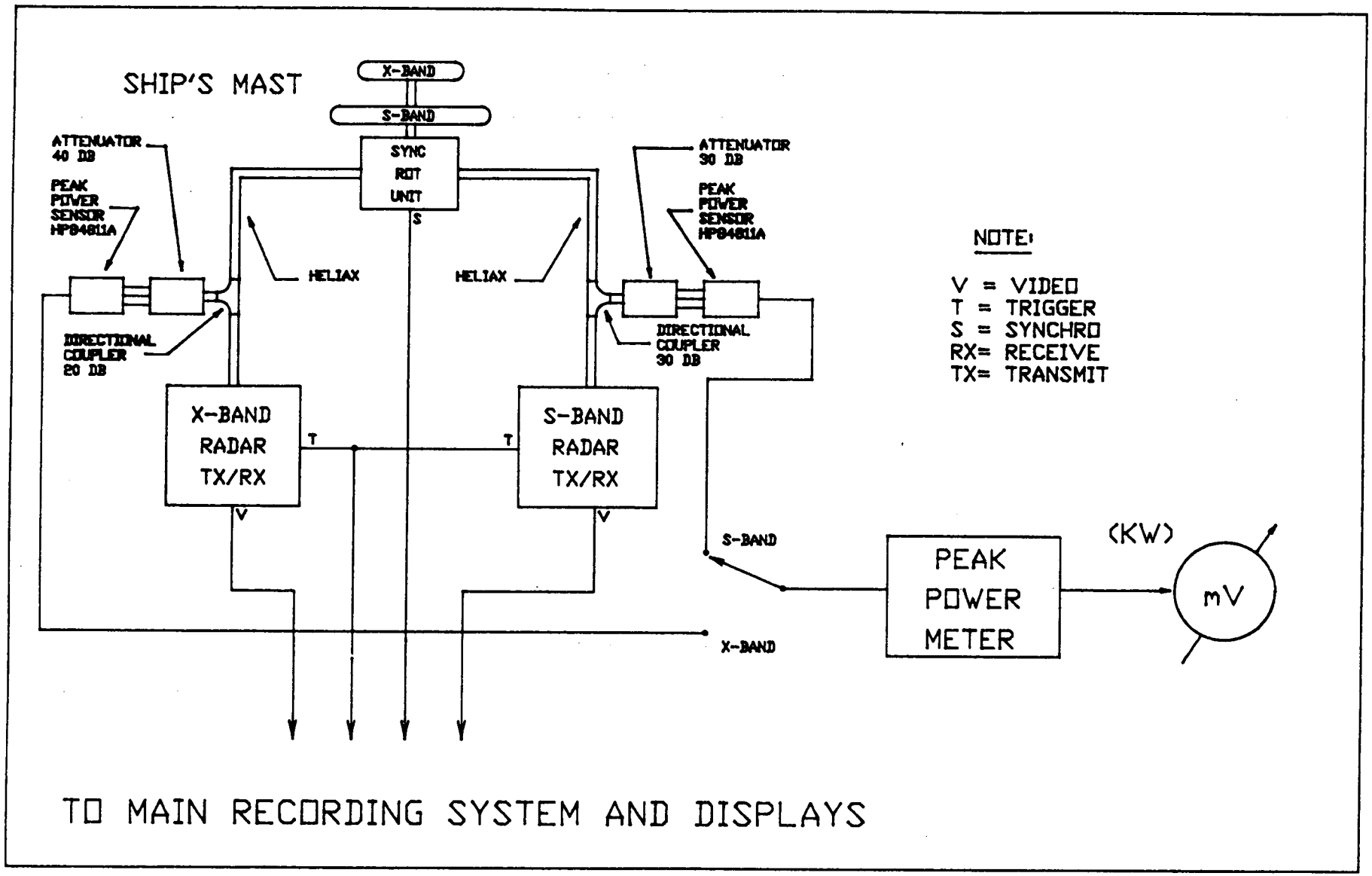

Figure 2.4 Configuration of transmitted power measurement.

2.4 COLLECTION OF DATA

Once installation and testing was complete, April 1985 was spent using the Racal/Decca 2459 F/I band radar system and the Viatec interface and recording system to assess iceberg detectability. A wide range of iceberg and environmental data was collected and is summarized briefly below. Sea-ice targets are specifically excluded

Icebergs:

- smallest: Berg 051, 4.6 m x 5 m x 1.5 m (LxWxH)
- largest: Berg 007, large dry dock, 130 m x 250 m x 63 m
- average size: Medium
- total measured 38.

The icebergs were classified in size using the WMO/AES classification given in Appendix 1.

The extremes of sea state and meteorological data for each of the following were:

- significant wave height 0 m to - 7 m
- wind speed 0 kt to - 35 kts
- visibility 0 naut mi - 25 naut mi
- air temperature -4.4°C to 3.6°C
- sea temperature -1.2°C to 0.2°C
- dew point temperature -8.0°C to 4.0°C
- barometric pressure 994.5 to 1027.5 mbar.

A complete set of environmental data was collected and is retained by Viatec Resource Systems Inc.

TABLE 2.2.
Ice and iceberg dimensions and classification.

Target designation	L_1 (m)	L_2 (m)	H (m)	Classification (based on WMO/AES classification)
BERG 001	110	110 est.*	26	MDD
BERG 002	97	74	29	MPI
BERG 003	14	14 est.*	2	BERGY BIT
BERG 004	NOT	MEASURED	-	ICEBERG
GRW 001	-	-	-	SEA ICE
GRW 002	9.2	7.7	.9	SEA ICE
GRW 003	-	-	-	SEA ICE
BERG 005	120	120 est.*	46.1	LPI
BERG 006	87	68	32	MWD
BERG 007	130	250	63	LDD
BERG 008	130	65	15	MPI
GRW 004	57	57 est.*	10	SDM

... continued ...

Table 2.2. continued...

GRW	005	60		60	est.*	10		SDD
GRW	006	-		-		-		SEA ICE
GRW	007	-		-		-		SEA ICE
BERG	009	36		51		11		SWD
BERG	010	NOT		MEASURED		-		MDD or 2 SDM
BERG	011	86.0		-		20		MDM
BERG	012	35		48		6.4		SDD
BERG	013	48		53		7.1		SDM
BERG	014	100		100	est.*	22		MWD
BERG	015	130		150		30		MBL
BERG	016	160		180		23	est.	LDD
BERG	017	110	est.	110	est.*	23	est.	MBL
BERG	019	180	est.	140		50		LDM
BERG	020	100		100	est.*	32		MBL
BERG	021	91		44		30		MBL
BERG	022(1)	3.1		3.1		1.2		SEA ICE
BERG	022(2)	3.1		3.1		1.2		SEA ICE
BERG	022(3)	7.7		3.1		1.2		SEA ICE
BERG	022(4)	6.2		3.1		1.5		SEA ICE
BERG	050	90		89		27		MBL
BERG	051	4.6		5.5		1.5		GROWLER
BERG	052	75		75	est.*	10		STA
BERG	053	64		51		11		SBL
BERG	054	NOT		MEASURED		-		ICEBERG
BERG	055	15		15	est.*	3.1		BERGY BIT
BERG	056	140		-		21		LTA
BERG	057	NOT		MEASURED		-		ICEBERG
BERG	058	15		15		4.6		BERGY BIT
BERG	059	130		130	est.*	41		MBL
BERG	060	69.4		75.5		15.5		MWD
BERG	061	12		-		4.0		SEA ICE
BERG	062	12		-		3.1		SEA ICE
BERG	063	11		-		4.3		SEA ICE
BERG	064	15		11		3.1		SEA ICE
BERG	065	15		-		2.5		SEA ICE
BERG	066	57		87		8.1		SDM
BERG	067	54		65		12		SBL
BERG	068	91		110		27		MPI
BERG	069	66		120		13		MDM
BERG	070	4.6		4.6	est.*	1.2		GROWLER
BERG	071	4.6		-		1.0		SEA ICE
BERG	072	4.6		2.5		-		SEA ICE
BERG	073	31		-		4.4		SEA ICE
BERG	074	6.1		-		1.8		SEA ICE
BERG	075	12		-		2.5		SEA ICE
BERG	076	7.7		-		1.8		SEA ICE
BERG	077	100		100	est.*	31		MPI

...continued...

Table 2.2 continued...

BERG 078	14	14	est.*	3.7	BERGY BIT
BERG 079	7.4	-		.9	SEA ICE
BERG 080	12	-		2.5	SEA ICE
BERG 081	12	-		1.2	SEA ICE
BERG 082	7.7	-		1.2	SEA ICE
BERG 083	80	80	est.*	20	MBL

* second dimension estimated to be the same as the measured dimension.

TABLE 2.3.
Summary of berg sizes

DESCRIPTION	QTY
Large icebergs	5
Medium icebergs	17
Small icebergs	9
Bergy bits	5
Growlers	2
Not measured	4
Iceberg total (measured)	38
Sea ice targets	23

3.0 DATA ANALYSIS

The aim of this study was to investigate the iceberg detection capability of shipborne marine radar. The objective included providing data for icebergs in sea clutter, with emphasis on the smaller iceberg sizes, and demonstrating the advantages of signal processing for improved detection capability.

The probability of detecting an iceberg with radar is highly dependent on the its size, shape, and aspect with respect to the radar, as well as the prevailing environmental conditions. The detectability of a particular iceberg may be quantified by directly measuring its blip-to-scan ratio (i.e., the ratio of the number of times a target exceeds a fixed threshold to the total number of scans on the target) or indirectly by measuring the received signal-to-clutter ratio. Although analysis of blip-to-scan and signal-to-clutter ratios for all targets was not possible, an analysis of representative events was carried out to provide insight into the detection process and to validate the use of a computer model to estimate iceberg detection capability. As a result this validated model may be used confidently to provide estimates of detection capability of radar for icebergs of various sizes in a variety of environmental conditions.

The analysis also contains an investigation into radar cross-sections of icebergs using X- and S-band radars. Whereas present sea clutter models are adequate for most cases, in selective analysis they can be extended using this data base to include more instantaneous clutter levels resulting from both wind speed and significant wave height. Also included is an investigation into the frequency dependence of the iceberg's radar cross-section using several representative icebergs.

The analysis of the digital radar data stored on magnetic tape during the field program was carried out using a PDP 11/23+ computer and hardware required to produce a 256 x 256-pixel colour display. The data of interest on each tape were identified from information found in the field log-books. Each recorded event contained summary information on the targets and environmental conditions present and was logged at the start of the event. Additional environmental and target verification information was collected in the form of photo's, slides and meterological data.

Radar data for each iceberg was recorded at test points located along inbound and outbound paths at intervals of about 1 naut mi (1.9 km). Each test point contains data for both X and S band radars for at least two pulse-length settings. Two data formats were used, one giving 360° data recording and the other providing a sector format. The sector format is superior for iceberg analysis while the 360° format is ideal for clutter analysis. The 360° recording format provides clutter data for the analysis programs in any required direction. The sector recordings provide 22.5° of data.

Each of the data tapes was subsequently logged into a data base that provides a listing of the data format (i.e., sector or 360°) and time and date of collection. Target data for a test point, radar, and pulse length of interest may be located easily and written onto disk for further analysis.

Once the data have been stored on disk, they are available for use with the analysis software. This software consists of programs that provide the following functions:

- Calibrate and plot processed or unprocessed data in A-scope format (i.e., amplitude versus range) as given in Figure 3.1 for a typical iceberg.

- display processed or unprocessed data in polar or rectangular co-ordinates on an RGB (Red Green Blue) monitor;

- alter interactively the display colour look-up tables;

- Average up to 32 scans of data; and

- produce time series and statistical analysis which includes the calculation of the mean and standard deviation as well as histograms of target and clutter power for a 64-s time series with a 2-s sample interval.

This software may be used in the assessment of iceberg signal-to-clutter ratios as well as the number of times a target was detected out of the total number of scans (referred to as the blip-to-scan ratio). Mean clutter and target signal strengths are obtained by averaging the data over 32 scans and by plotting received power as a function of range. This received power may be compared directly to that predicted by a computer model (Ryan 1985; Ryan et.al. 1985) or another similar program may be used to convert the power received into a radar cross-section.

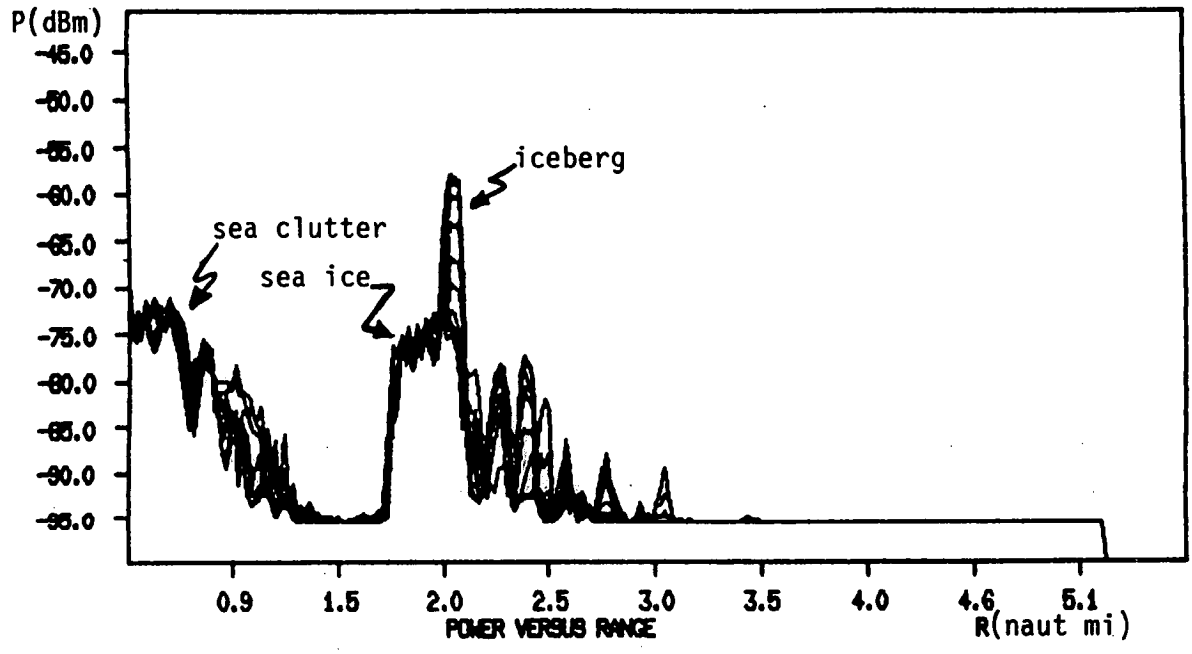

Figure 3.1: **Averaged S-band data of an iceberg and two types of clutter. Multiple traces represent adjacent radar sweeps.**

4.0 RESULTS

4.1 CALIBRATED TARGET DATA

The radar systems were calibrated from the receiver input to the recording system and the results are summarized in Appendix 2. It was necessary to close this calibration using a calibrated reference target having a known radar cross-section. This direct calibration ensures that all system losses and antenna gains have been assessed properly. Although received signals from this target exhibited quite large fluctuations with time, the average over 32 scans (64 s) shows excellent agreement with theoretical values. Table 4.1 presents measured received power and predicted power for the target. The target was a Luneburg lens (omni-azimuth) having a 10-m^2 cross-section at X-band and a 1.2-m^2 cross-section at S-band. Figures 4.1 and 4.2 show plots of measured and predicted received power. The model used to calculate received power incorporates a propagation factor that takes into account multi-path and ocean roughness (Blake 1980; Ryan 1985). The propagation factor is quite sensitive to target height especially at the transition from R^{-4} to R^{-8} range dependency. This transition range is at a greater range for X-band as compared to S-band and does not affect the calibrated data for X-band. However, the three plots in Figure 4.2 indicate that varying the target height from 2 to 4 m for S-band has a major effect on the received power. The best agreement was obtained at 3 m which was the actual tareget height with a significant wave height of 1 m. Agreement between the calibrated target data and predicted (theoretical) values indicate that quantitative measurements of received power from the data is possible.

Table 4.1. Comparison of measured received power from a calibrated reference target to predicted received power using computer model.

Range naut mi (km)	X-BAND RECEIVED POWER (dBm)	
	Data (Tape 71)	Model
1.6 (3.0)	- 45	- 56
2.1 (3.9)	- 53	- 55
2.8 (5.1)	- 55	- 55
3.3 (6.1)	- 59	- 59

Range naut mi (km)	S-BAND RECEIVED POWER (dB m)	
	Data (Tape 70)	Model
0.5 (0.9)	- 56	- 54
1.6 (3.0)	- 65	- 64
2.2 (4.1)	- 69	- 68

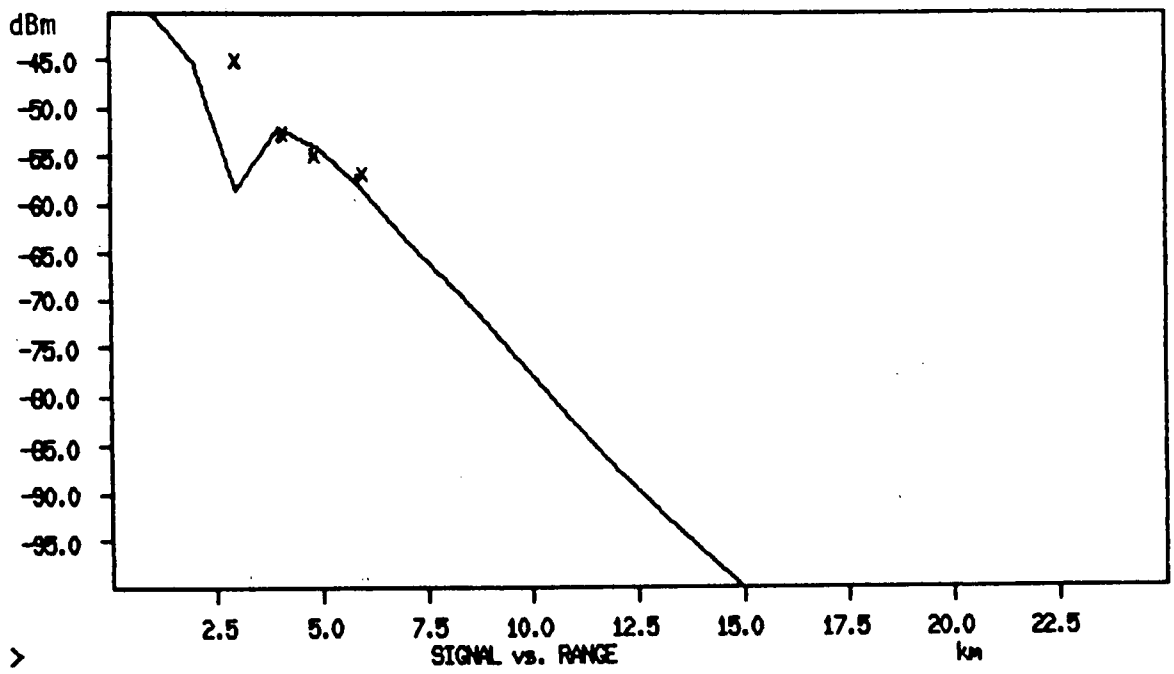

Figure 4.1: X-band calibrated target data compared to model output.

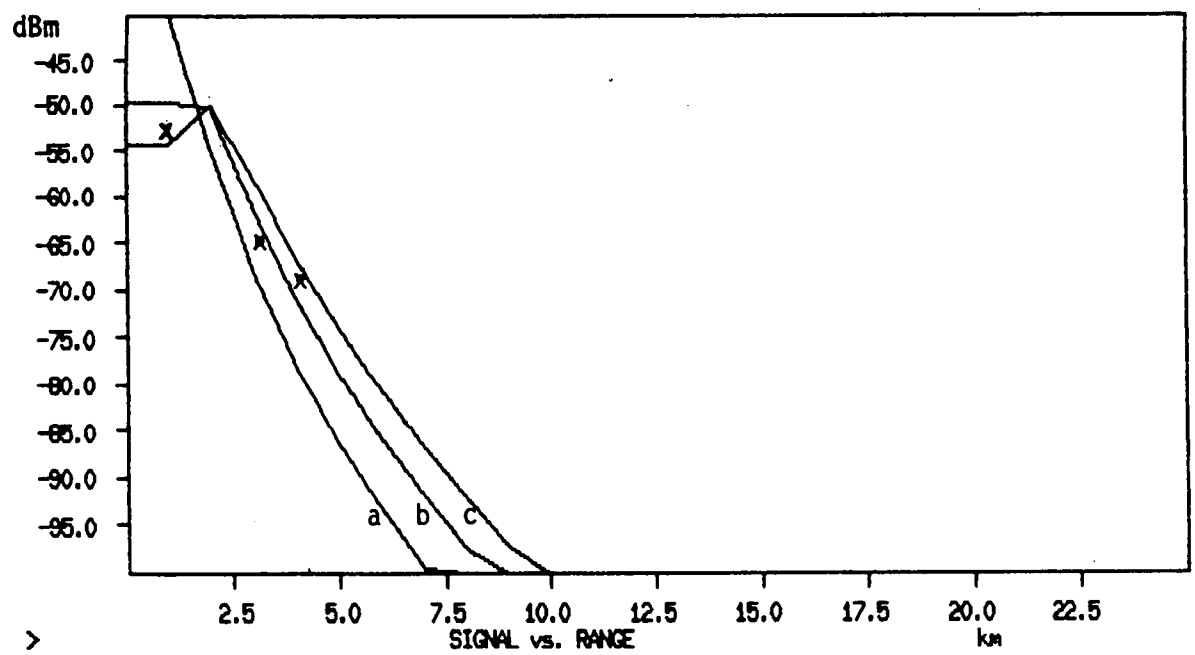

Figure 4.2: S-band calibrated target data compared to model output for three target heights.

(a) h = 2 m
(b) h = 3 m
(c) h = 4 m

4.2 SEA CLUTTER

The most dominant factor influencing iceberg detection is the presence of sea clutter. There were several cases during the data collection program when icebergs could be detected outside the clutter region but were "lost" when approached by the ship. There were also cases when smaller pieces of ice were never detected on the radar but could be identified visually. These specific cases may be analysed to assess a particular iceberg's detectability in clutter, however, this analysis would probably be too specific to be applied to a general iceberg population. It is, therefore, important to develop and refine models that will provide probabilities of detection for average icebergs (within size classes) in average sea clutter (by sea state). The data base that has been collected contains many valuable sea clutter data for significant wave heights from 0.3 m to 7 m and various wind speeds. A sample of these data is presented here and comparisons are made to some presently used models. Good agreement was obtained between the X-band data and the data of Nathanson (1969) and whereas S-band showed general agreement, much wider variations were noted between data sets having the same environmental conditions. Figures 4.3 through 4.7 present X-band sea clutter data expressed in normalized radar cross-sections, σ^o, as a function of grazing, angle and show comparisons with the models of Nathanson (1969) and Sittrop (1977). The normalized cross-section for the sea clutter was calculated by inverting the standard radar equation 1970 Skilnik p. 2-4, equation 1, where the propagation factor is assumed to be one. In general, a good agreement between the collected data and Nathanson's is obtained. The Sittrop model does not appear to provide representative values especially when high seas exist (see Figure 4.4 and 4.6). Figure 4.7 compares three sets of data taken on different days for a significant wave height of 3 m. The only differences in the data are the wind speed and the direction. Although the lowest clutter is obtained for a 10-kt 45° downwind, a 13-kt 45° upwind on a different day is only a few dB greater. The highest clutter in this figure was for the 23-kt wind. Figure 4.7 illustrates that the dependence of sea clutter on wind speed at X-band is subtle in comparison to the effect of significant wave height (compare Figure 4.3 and Figure 4.5). Note, that Nathanson (1969) did not provide for data up to a significant wave height of 4.5 m and his data are only for grazing angles of 0.1, 0.3, and 1.0 degrees. The curves plotted in Figure 4.6 and later in Figure 4.11 were obtained by extrapolating Nathanson's data, which was implemented in Viatec's radar model. The Sittrop model provides best agreement when conditions of a fully developed sea exist. Figures 4.8 through 4.12 present sea clutter data at S-band (for the same data collection times as Figures 4.3 through 4.7).

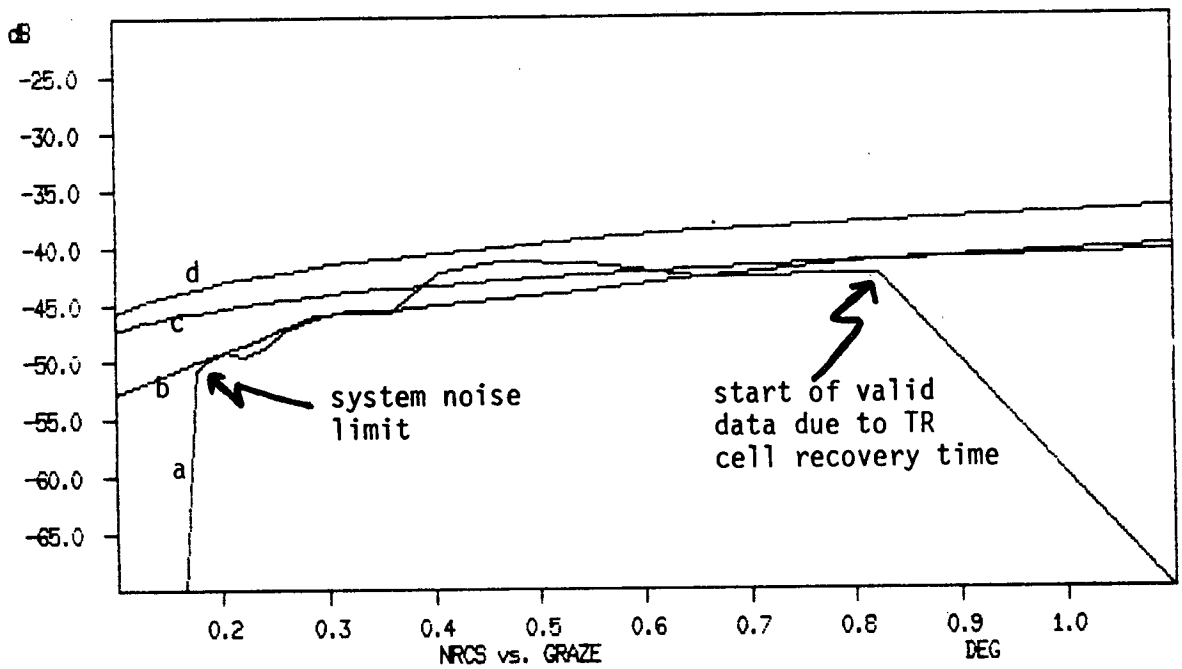

Figure 4.3 Normalized radar cross-section at X-band for the ocean with 1.0 m significant wave height and 20-kt wind and comparison with models.

(a) Data for SWH = 1 m, 45° upwave
WS = 20-kt, upwind.
(b) Nathanson
(c) Sittrop cross-wind.
(d) Sittrop upwind.

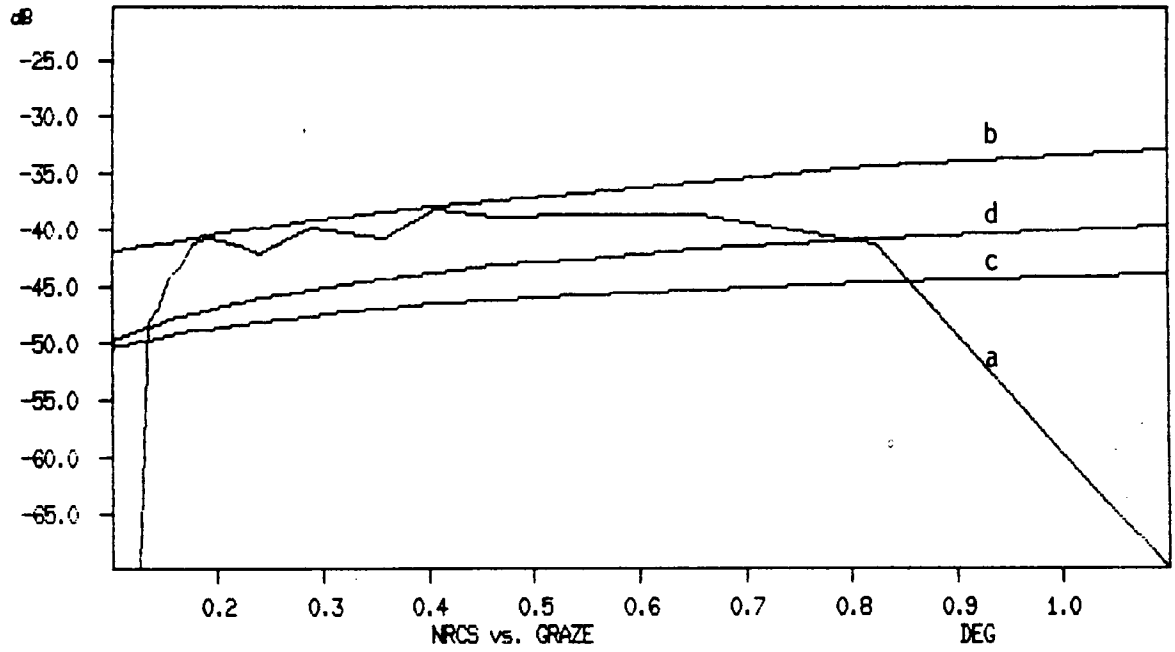

Figure 4.4: Normalized radar cross-section at X-band for the ocean with 2.5 meter significant wave height and 16-kt wind and comparison with models.

(a) Data for SWH = 2.5 m, 45° upwave
WS = 16-kt, downwind.
(b) Nathanson.
(c) Sittrop cross-wind.
(d) Sittrop upwind.

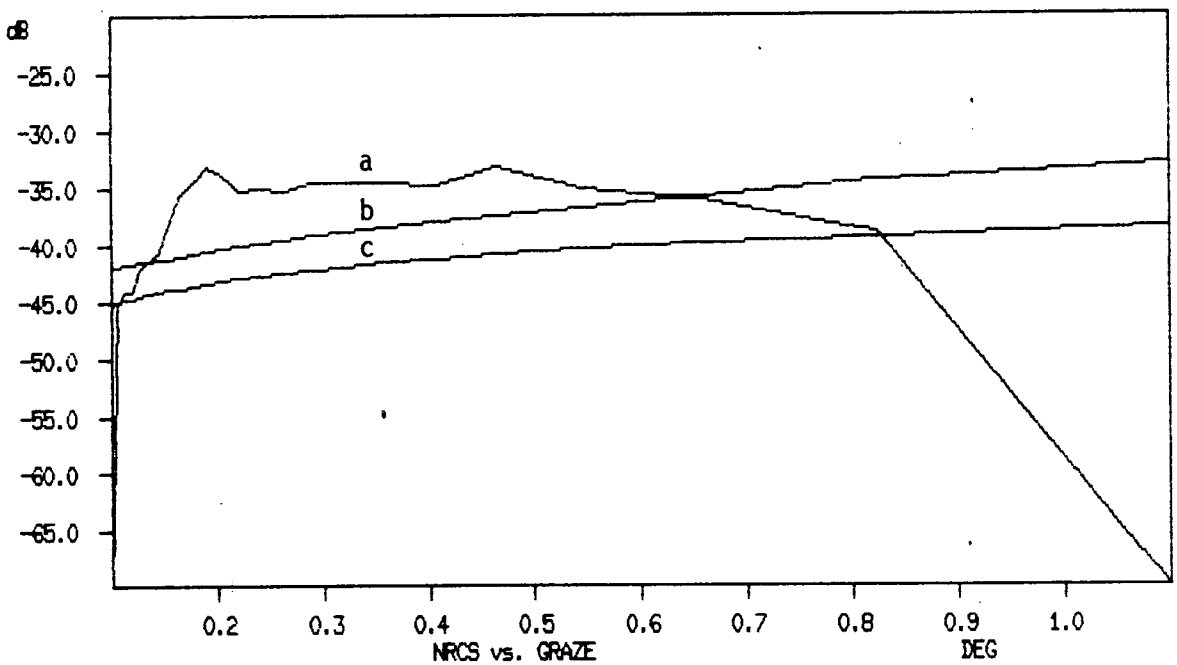

Figure 4.5: Normalized radar cross-section at X-band for the ocean with 3.0 m significant wave height and 23-kt wind and comparison with models.

(a) Data for SWH = 3.0 m, cross-wave
WS = 23-kt, 45° downwind.
(b) Nathanson.
(c) Sittrop cross-wind.

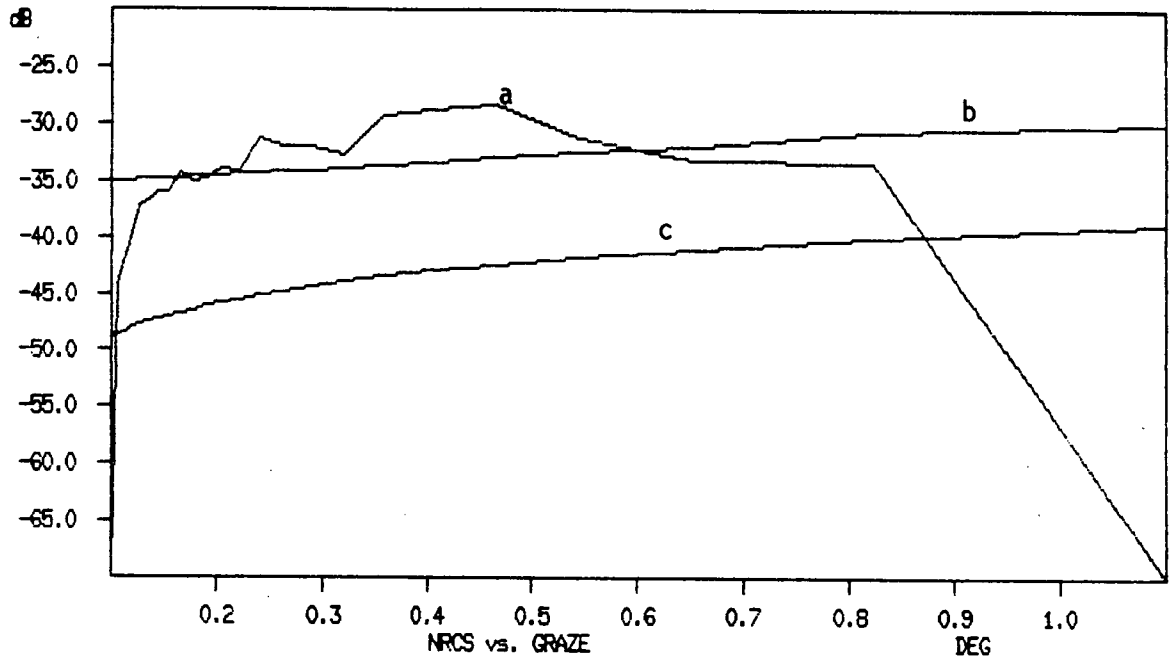

Figure 4.6: Normalized radar cross-section at X-band for the ocean with 4.5 m significant wave height and 17-kt wind and comparison with models.

(a) Data for SWH = 4.5 m, upwave
WS = 17-kt, upwind.
(b) Nathanson.
(c) Sittrop upwind.

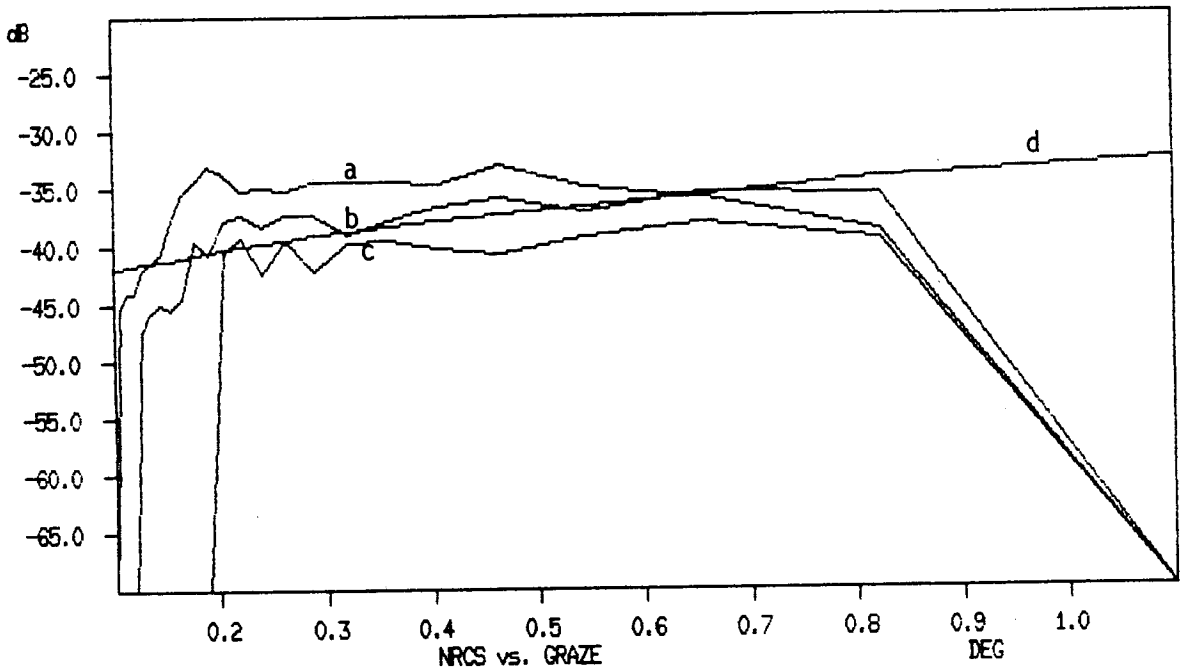

Figure 4.7: Normalized radar cross-section at X-band for the ocean with 3.0 m significant wave height and wind speeds of 10, 13, and 23-kt and comparison with model.

(a) Data for SWH = 3.0 m, cross-wave
WS = 23-kt, 45° upwind.
(b) Data for SWH = 3.0 m, cross-wave
WS = 13-kt, 45° upwind.
(c) Data for SWH = 3.0 m, 45° cross-wave
WS = 10-kt, upwind.
(d) Nathanson.

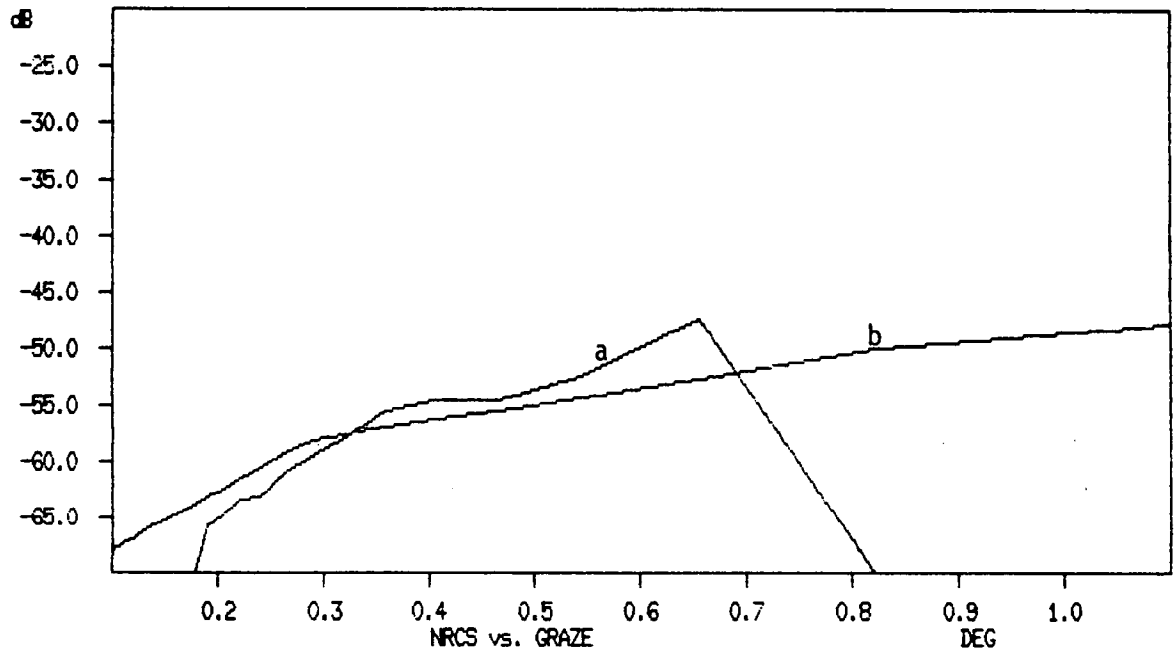

Figure 4.8: **Normalized radar cross-section at S-band for the ocean with 1.0 m significant wave height and 20-kt wind and comparison with model.**

(a) Data for SWH = 1.0 m, 45° upwave
WS = 20-kt, upwind.
(b) Nathanson.

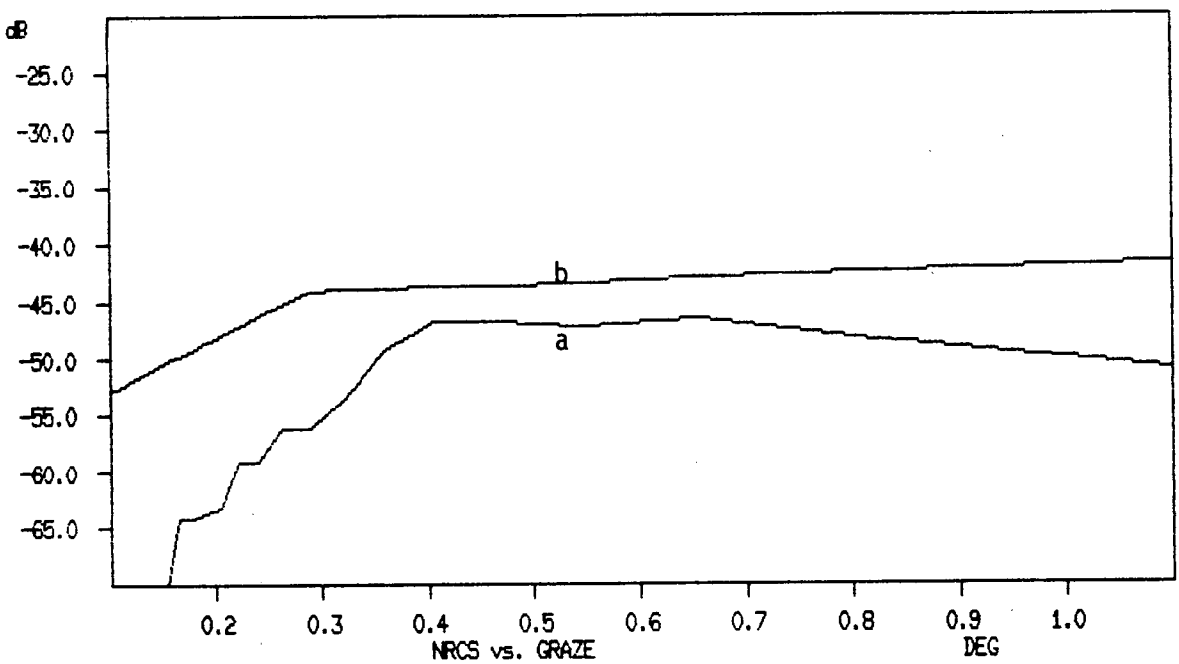

Figure 4.9: **Normalized radar cross-section at S-band for the ocean with 2.5 m significant wave height and 16-kn wind and comparison with model.**

(a) Data for SWH = 2.5 m, 45° upwave
WS = 16-kt, downwind.
(b) Nathanson.

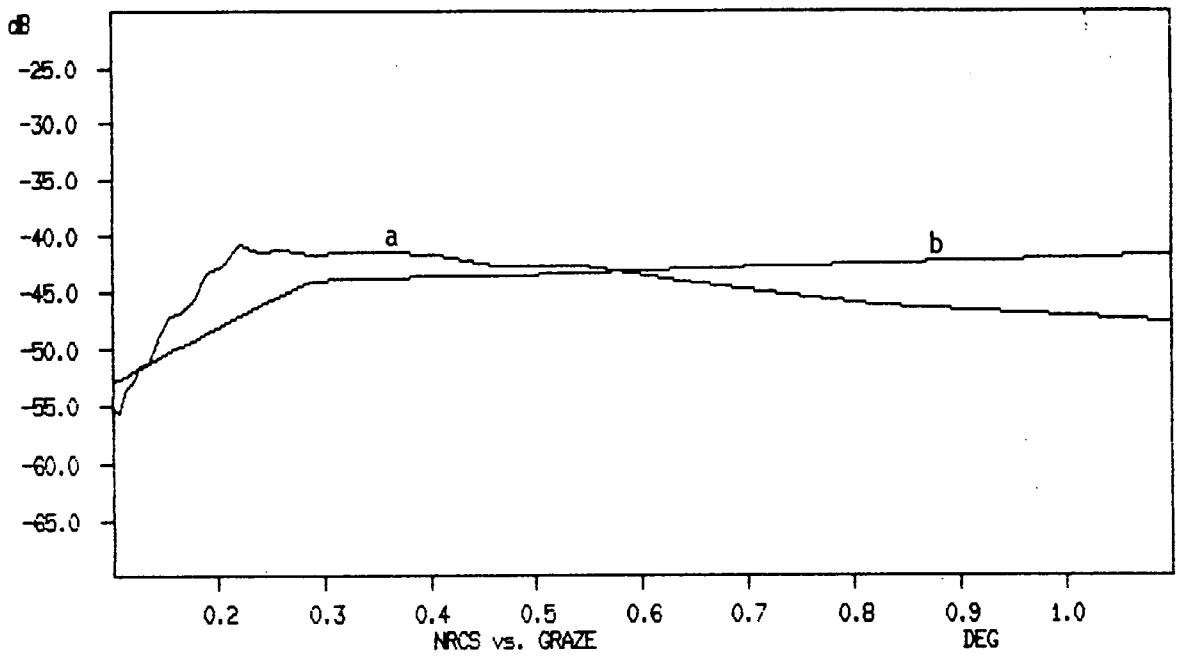

Figure 4.10: **Normalized radar cross-section at S-band for the ocean with 3.0 m significant wave height and 23-kt wind and comparison with model.**

(a) Data for SWH = 3.0 m, cross-wave WS = 23-kt, 45° downwind.

(b) Nathanson.

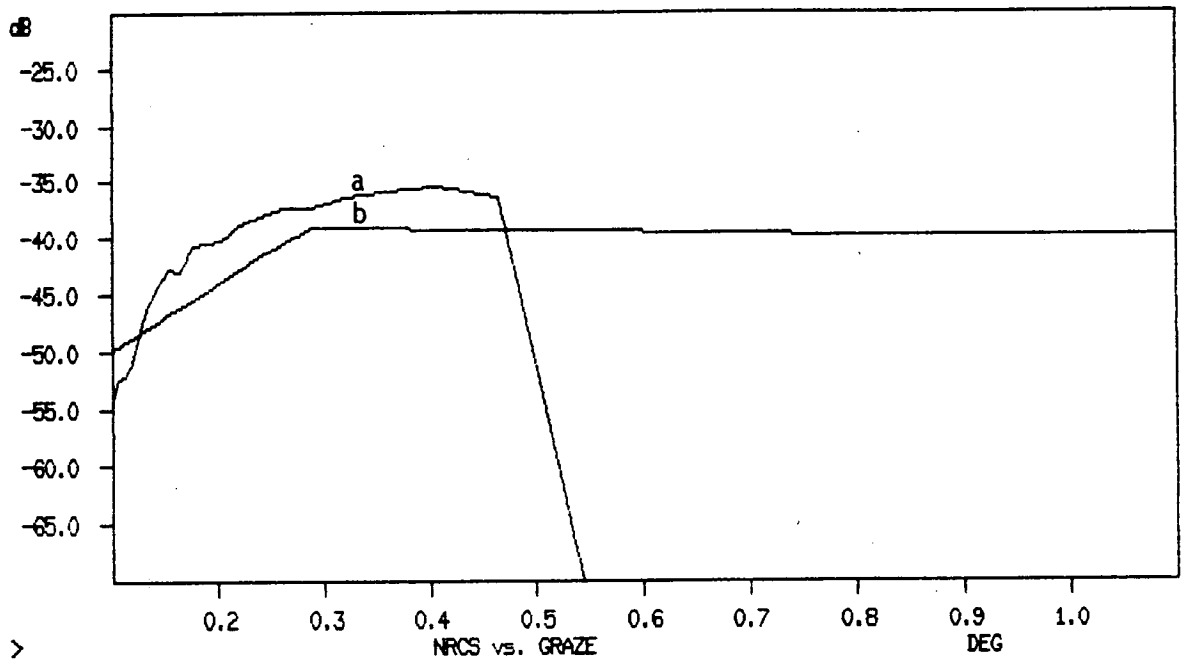

Figure 4.11: Normalized radar cross-section at S-band for the ocean with 4.5-m significant wave height and 17-kt wind and comparison with model.

(a) Data for SWH = 4.5 m, upwave
WS = 17-kt, upwind.

(b) Nathanson.

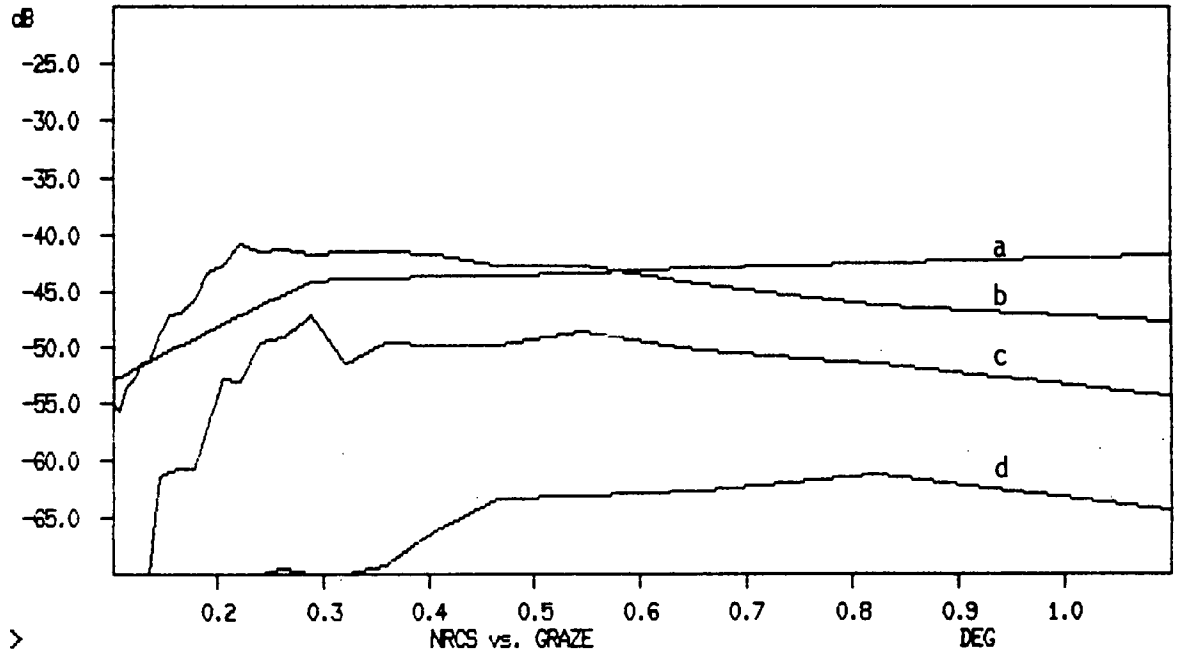

Figure 4.12: Normalized radar cross-section at S-band for the ocean with 3.0 m significant wave height and wind speeds of 10, 13, and 23-kt and comparison with model.

(a) Nathanson.
(b) Data for SWH = 3.0 m, cross-wave
WS = 23-kt, 45° downwind.
(c) Data for SWH = 3.0 m, cross-wave
WS = 13-kt, 45° upwind.
(d) Data for SWH = 3.0 m, 45° cross-wave
WS = 10-kt, upwind.

The S-band sea clutter shows more variability when comparing data from the same significant wave height (Figure 4.12), which seems to indicate that the wind/swell direction plays a fairly large role in the generation of clutter at S-band. This point needs further analysis to quantify the effects.

In general, it appears from these limited data that the use of Nathanson's data in an X-band sea clutter model will provide a good estimate of actual clutter levels. The S-band data show much more variability and, therefore, the Nathanson data should be used only until a better model becomes available. It appears that the Nathanson data usually give greater than, or equal, clutter compared to the measured data and will, therefore, provide pessimistic estimates of iceberg detectability.

However, the broad range of data available within this data base represent the possibility of expanding Nathanson's data to include the effects of wind/swell direction as well as higher sea states.

4.3 RADAR CROSS-SECTION OF ICEBERGS

The radar cross-section of an iceberg is highly dependent on iceberg size, and shape, and orientation. Icebergs, the dimensions of which fall within the same classification group (i.e., small, bergy bit, etc.), may exhibit a wide range of cross-section values and the cross-section of each iceberg will vary depending on its orientation with respect to the radar. The following analysis of representative data provides quantitative measurements of radar cross-sections of icebergs at X- and S-band. The measured values for X-band are compared to available models and the S-band cross-sections are presented alone.

The computer model used to calculate iceberg signal strength (Ryan 1985; Ryan et.al. 1985), is based on the theory of microwave propagation over a rough sea as presented by Blake (1980). The model takes into account that an iceberg is not a point target and, therefore, to allow for propagation effects, the reflected electric field must be averaged over the iceberg's height. The model has been shown, in section 4.1, to provide excellent agreement with calibrated target data. The procedure for extraction of the iceberg's radar cross-section from the data was to obtain received power for each range (average of 32 radar scans at each test point) and to perform an interactive procedure to find the best-fit predicted curve by varying only the iceberg's normalized radar cross-section, σ°. The radar cross-section, σ, is then given by equation 4.1:

$$\sigma = \sigma^\circ A \qquad (4.1)$$

where A is the area of the iceberg projected towards the radar.

Figures 4.13 and 4.14 show plots of predicted received power with actual data points superimposed. The data are for a small blocky iceberg with above-water dimensions of height 7 m, length 48 m and width 53 m (Berg 013). The data were taken on a clear day with significant wave height of 3 m and a 13-kt wind. Figure 4.13 for X-band (1.0 μs pulse length) shows the best-fit, normalized radar cross-section, $\sigma^{\prime}_{o}$, to be about 0.14 (-9 dB), which, using equation 4.1, gives a radar cross-section of about 50 m^2. Figure 4.14 for the same iceberg at S-band gives a best fit $\sigma^{\prime}_{o}$ of 0.014, a factor of 10 less than X-band, for a cross-section of 5 m^2. As was found with the calibrated target data the S-band radar is quite sensitive to target height. Figure 4.14 gives predicted received power for 3 different iceberg heights. The 11 m height provides the best agreement. This problem is therefore identified as probably resulting from either an error in height measurement, or the effect of iceberg/swell interaction, or a combination of both. All of the data analysed fell within the range of these values, with X-band tending to have radar cross-sections up to about 10 dB (10 times) greater than S-band. Table 4.2 lists the other icebergs analysed in this manner and their radar cross-sections. This method of extracting average radar cross-sections is expected to be quite accurate as it ensures that any propagation anomaly can be identified. The average, normalized radar cross-section over the three iceberg sizes in Table 4.2 are 0.1 (-10 dB) for X-band and 0.03 (-15 dB) for S-band.

TABLE 4.2
Radar cross-sections of selected icebergs

Iceberg Class	Shape	Iceberg I.D.	Size (m) L x W x H			X-band $\sigma^{\prime}_{o}$	X-band (m^2)	S-band $\sigma^{\prime}_{o}$	S-band (m^2)
Small	Blocky	013	53	48	7	0.14	50	0.014	5
Small	Tabular	012	48	35	6	0.10	24	0.05	12
Medium	Blocky/wedge	008	126	65	15	0.05	72	0.012	17
Medium	Wedge	050	90	89	28	0.09	219	0.018	45
Large	Blocky	016	183	162	53	0.15	1371	0.06	549

Although the analysis of five icebergs does not provide comprehensive results, the radar cross-sections do agree with existing models for X-band. A review of existing models, Ryan (1985), presents the work of Dawe (1985) and Lowry et.al. (1984). Dawe gives a normalized radar cross-section value of -11 dB for blocky and tabular icebergs and -18.5 dB for other types, while Lowry et.al. (1984) present values for dry (-11 dB) and wet (-19 dB) icebergs. As most of the icebergs in Table 4.2 were blocky or tabular, the -11 dB value of Dawe is in good agreement. Further analysis of other icebergs within the data set is required to validate the range of cross-sections.

The normalized radar cross-section values at S-band cannot be compared to any existing model. However, it appears that -15 dB is quite representative of the data in Table 4.2 and it is physically reasonable to assume that the S-band cross-section would be less than X-band.

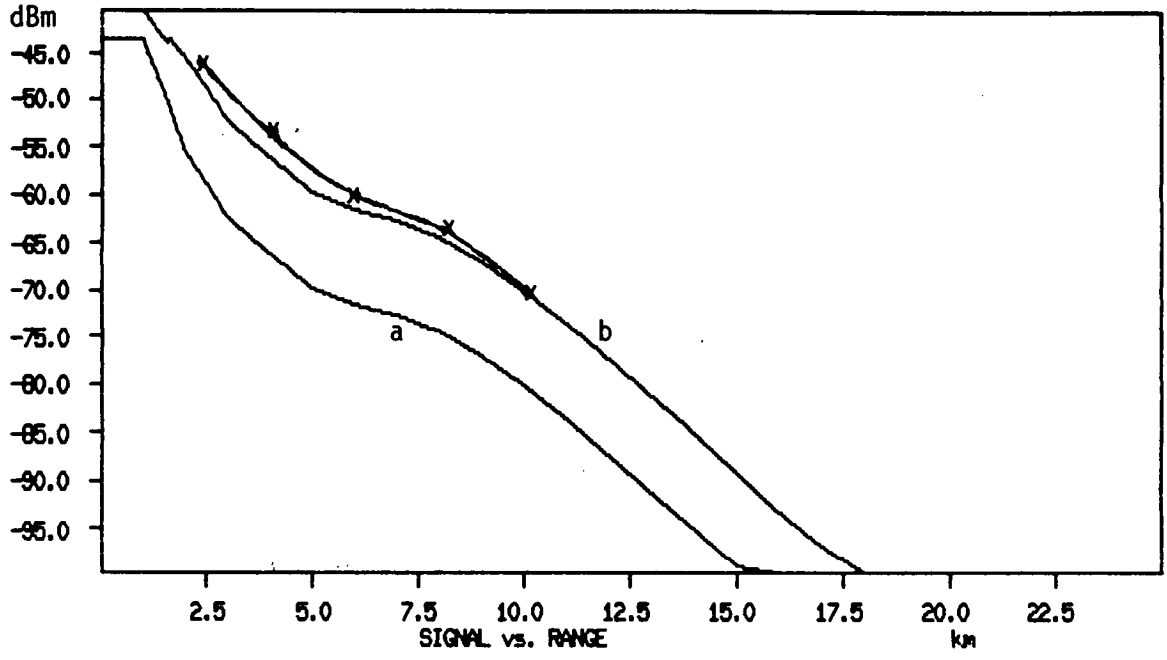

Figure 4.13: Predicted received power as a function of range for an X-band radar with long pulse, with actual received power superimposed for:

(a) $\sigma'_0 = 0.014$.

(b) $\sigma'_0 = 0.14$.

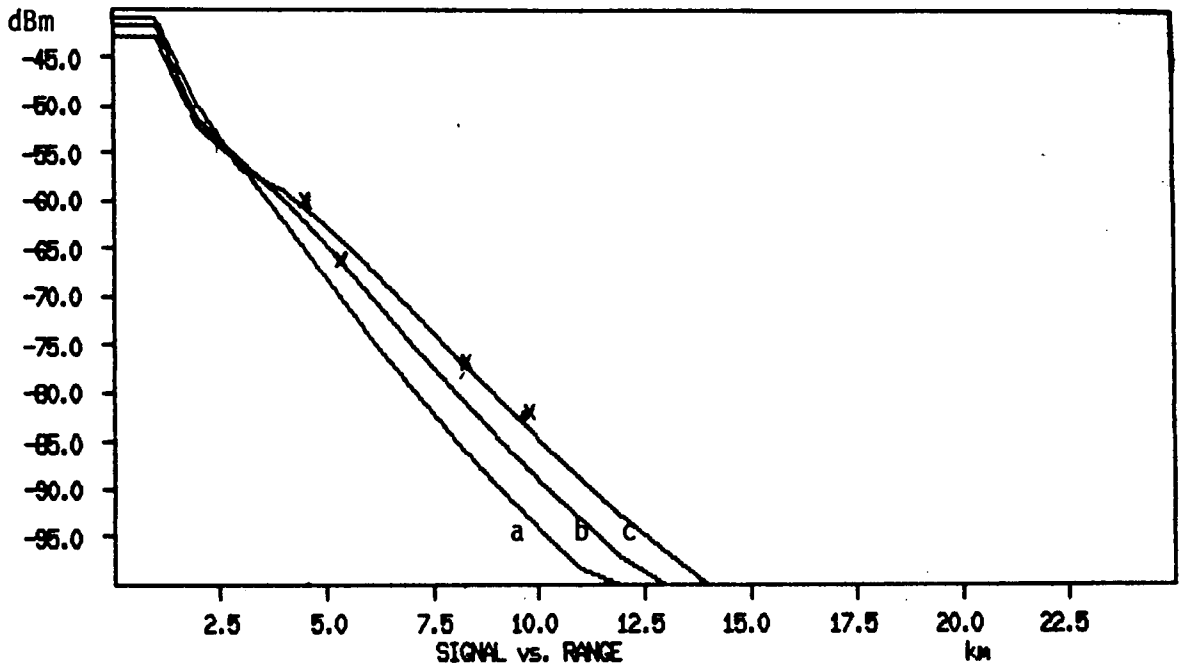

Figure 4.14: Predicted received power as a function of range fpr am S-band radar with long pulse, with actual data points superimposed. The three curves represent target heights of:

(a) h = 7.1 m
(b) h = 9.1 m
(c) h = 11.1 m

and σ'_0 = 0.014.

Note that changing σ'°, as in the previous figure, will not change the curve shape.

4.4 PROBABILITY OF DETECTION

The probability of detecting an iceberg target is a function of the ratio of target signal to background clutter (or interference) signal. When models for target signal and clutter have been assembled and validated, as in sections 4.1 and 4.2, it is possible to predict the probability of detecting a certain iceberg given the prevailing environmental conditions and knowing the associated statistical distributions.

Although the instantaneous signal-to-clutter ratio and, hence, probability of detection (Pd) (i.e., detection on one pulse) may vary significantly, if enough independent measurements of the signal-to-clutter ratio (S/C) for a particular target are made then an average S/C may be obtained and Pd derived from known curves relating S/C to Pd (Skolnik 1970). Alternatively, the well-established technique of blip-to-scan analysis may be used. The blip-to-scan analysis entails the setting of a received power threshold above which a signal is declared a target. The ratio of the number of times the actual target exceeded the threshold to the number of scans is the blip-to-scan ratio and is equivalent to the probability of detection. It is also necessary to count the number of false alarms (i.e., the number of times interference signals from clutter or noise exceed the threshold) which occur in the same period and form a probability of false alarm (Pfa) by calculating the ratio of the number of false alarms to the number of opportunities for a false alarm.

Most models predict probability of detection by calculating a mean signal-to-mean clutter ratio and use this ratio to derive a probability of detection assuming a Pfa (typically 10^{-6}) and target fluctuation model (Swerling 1 is often used for slow-moving targets at sea). The sets of curves presented by Skolnik (1970) are often used for this purpose although a computer model may be implemented (Ryan 1985).

The following analysis considers two detection examples for a small berg in sea clutter using an X-band radar. The data are analysed to provide probability of detection using blip-to-scan techniques and this is compared to the model output. The improvement of Pd by scan-to-scan averaging is presented as well as histograms of target, clutter, and target-plus-clutter-power.

4.4.1 Blip-to-Scan-Analysis

To evaluate the blip-to-scan ratio the raw data were plotted over 64 radials and a threshold level was identified. Figure 4.15 shows a calibrated plot of these radials with an arbitrary threshold superimposed. The target was at 2.3 naut mi and just exceeds the threshold. There are also several false alarms caused by clutter. These data represent one antenna scan past the target. Figures 4.16 to 4.23 present all 32 available data scans. The blip-to-scan ratio for this threshold is 18/32 or 0.56 with 13 false alarms, corresponding to a Pd of 56% and a Pfa of 1.6×10^{-4} (there are 13 false alarms and 10 radials x 256 pixels x 32 scan possibilities for a false alarm). The output of the model for this case is given in Figure 4.24 where the actual target position has been identified (4.3 km or 2.3 naut mi) and the S/C at that range is about 17 dB. A normalized radar cross-section of -11 dB is assumed. A plot of the average of the 32 scans given in Figures 4.16 to 4.23 is presented in Figure 4.25 and the S/C is about 19 dB. The model therefore shows very good agreement with the actual data and the 2-dB difference can be identified as the difference in actual radar cross-section (see Table 4.2) and assumed radar cross-section. Figure 4.26 presents the plot of Pd for the same iceberg as a function of range. The Pd at 4.3 km (2.3 naut mi) is 80%. If we use the actual measured radar cross-section as given in Table 4.2, the Pd is given in Figure 4.27 at about 87%.

An apparent discrepancy between the measured Pd of 56% using blip-to-scan analysis and the model prediction of 87% can be accounted for by considering the deviation of the clutter statistics from the Gaussian distribution assumed in the model.

It is believed that averaging (or integrating) as few as two radar scans will have the effect of normalizing the clutter probability distribution, thereby making the model valid when some scan-to-scan averaging or integration is assumed.

North (1963) discusses the "Central Limit Theorem" as it applies to the statistics of thermal noise. As the distributions of the clutter from consecutive scans approaches a normal (Gaussian) distribution, which is probably true in this case except for some of the clutter spikes extending the tail of the distribution, then the Central Limit Theorem with negligible error for as few as two scans. It is expected that for low-resolution data, such as the 1 us pulse (150 m range resolution) data presented here, this assumption is valid and permits use of the model with some degree of confidence. Even when no hardware scan to scan integration occurs a skilled operator often provides several seconds of scan-to-scan integration, (Blake 1980) both in the eye and memory.

The preceeding analysis demonstrates how models may be used effectively to provide good estimates of radar performance. However, what is not considered in this analysis is just how much the detectability is increased by scan to scan averaging.

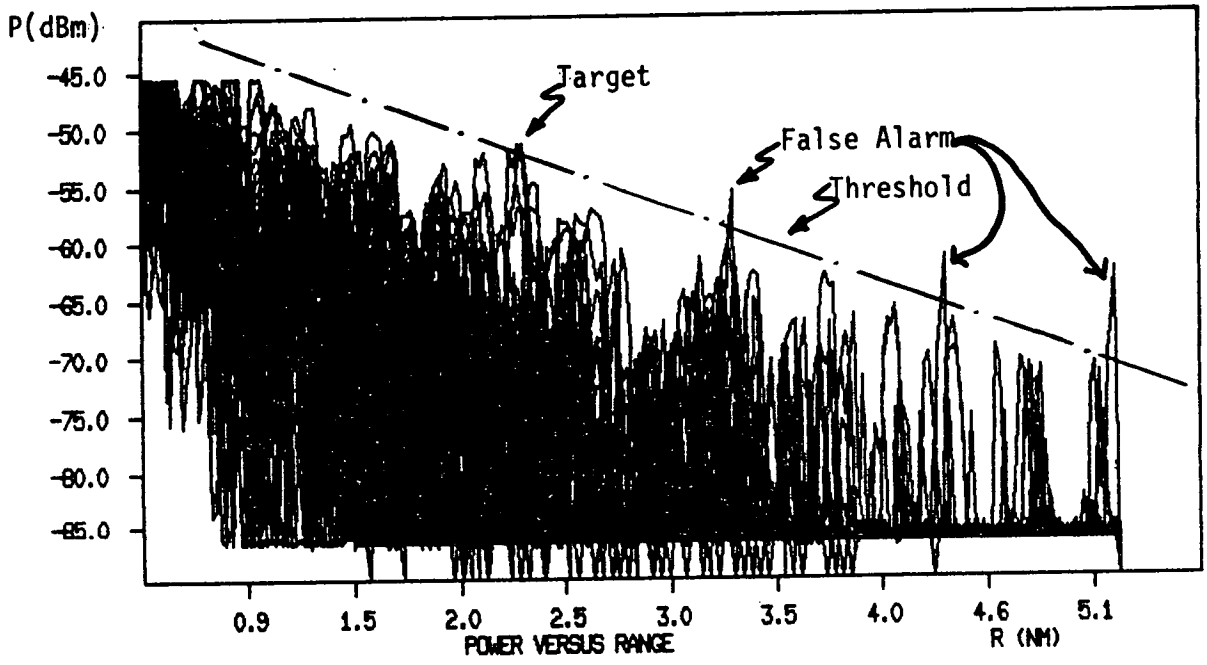

Figure 4.15: X-band radar data for a SDM in sea clutter (SWH = 3 m, WS = 13-kt).

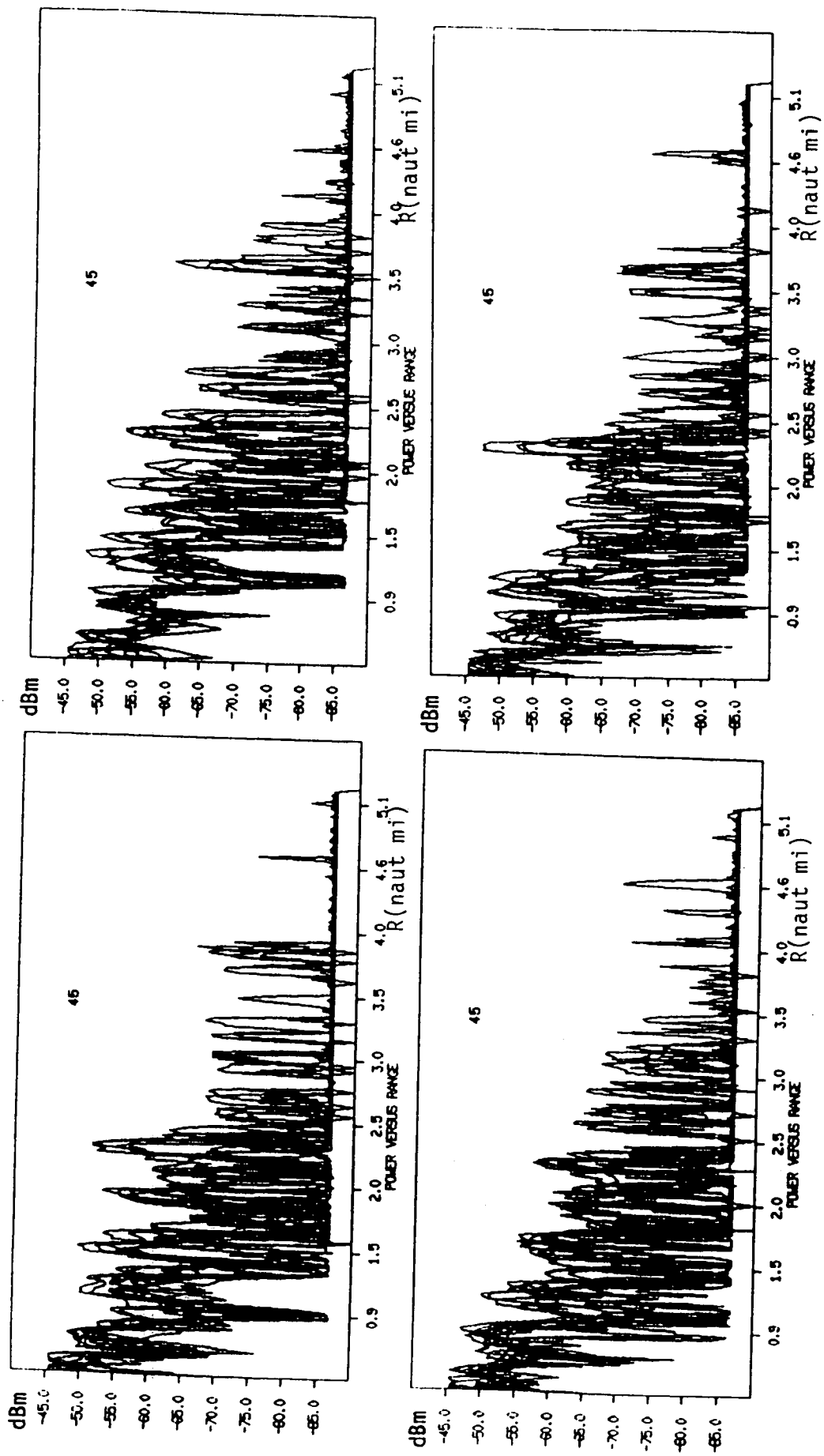

Figure 4.16 Received power data for berg 013, raw data, no averaging, scans 1 - 4.

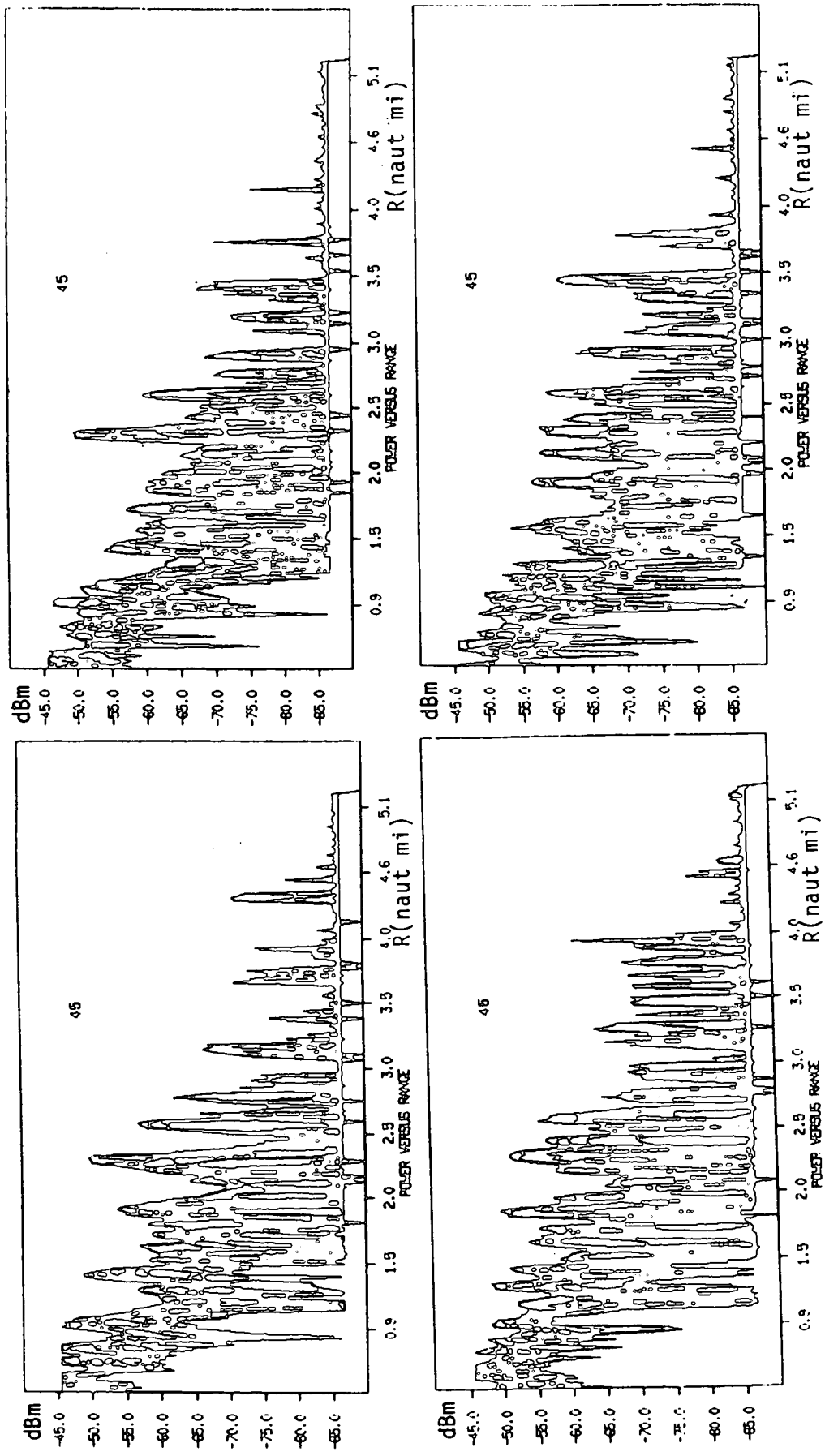

Figure 4.17 Received power data for berg 013, raw data, no averaging, scans 5 - 8.

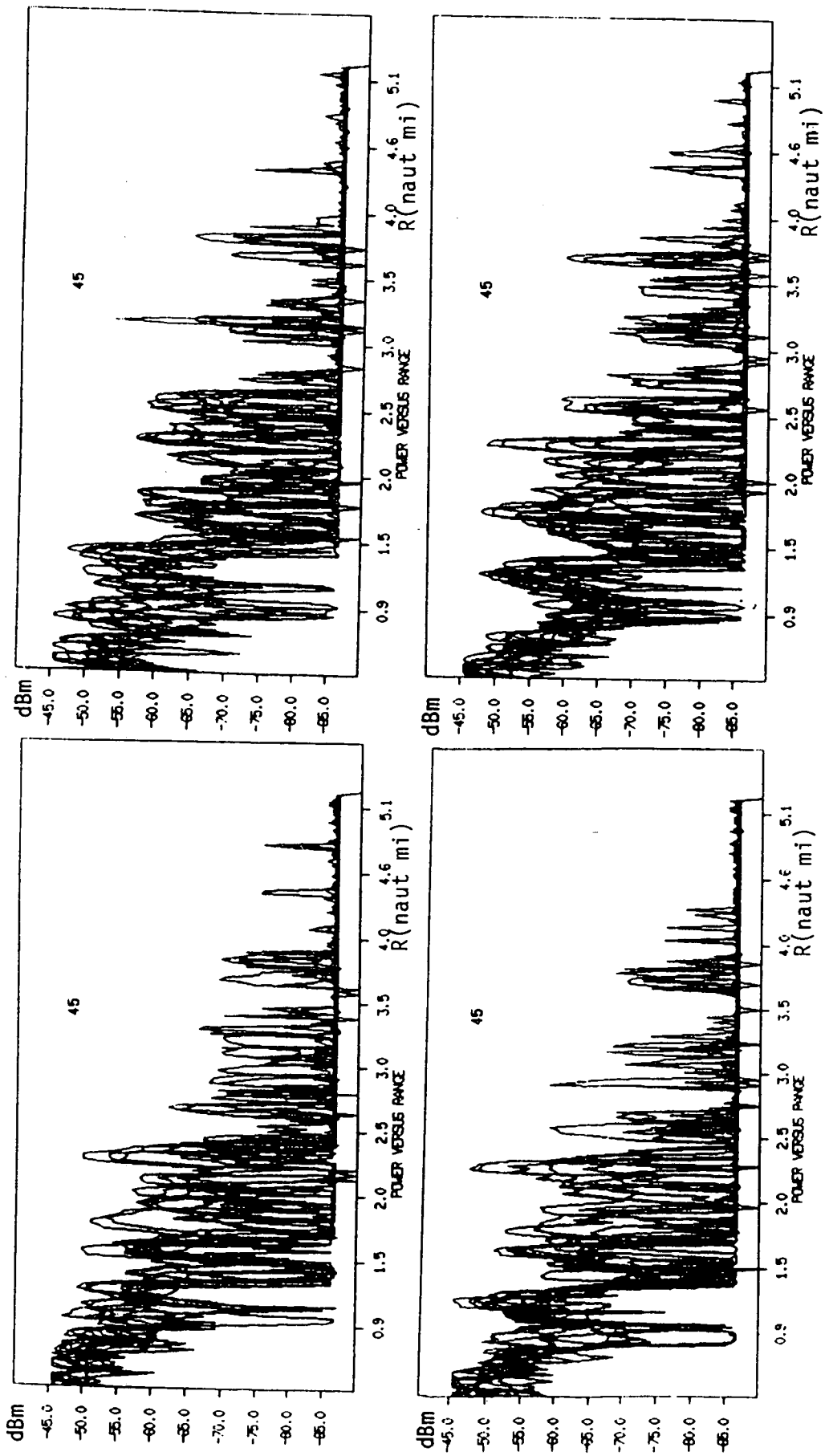

Figure 4.18 Received power data for berg 013, raw data, no averaging, scans 9 - 12.

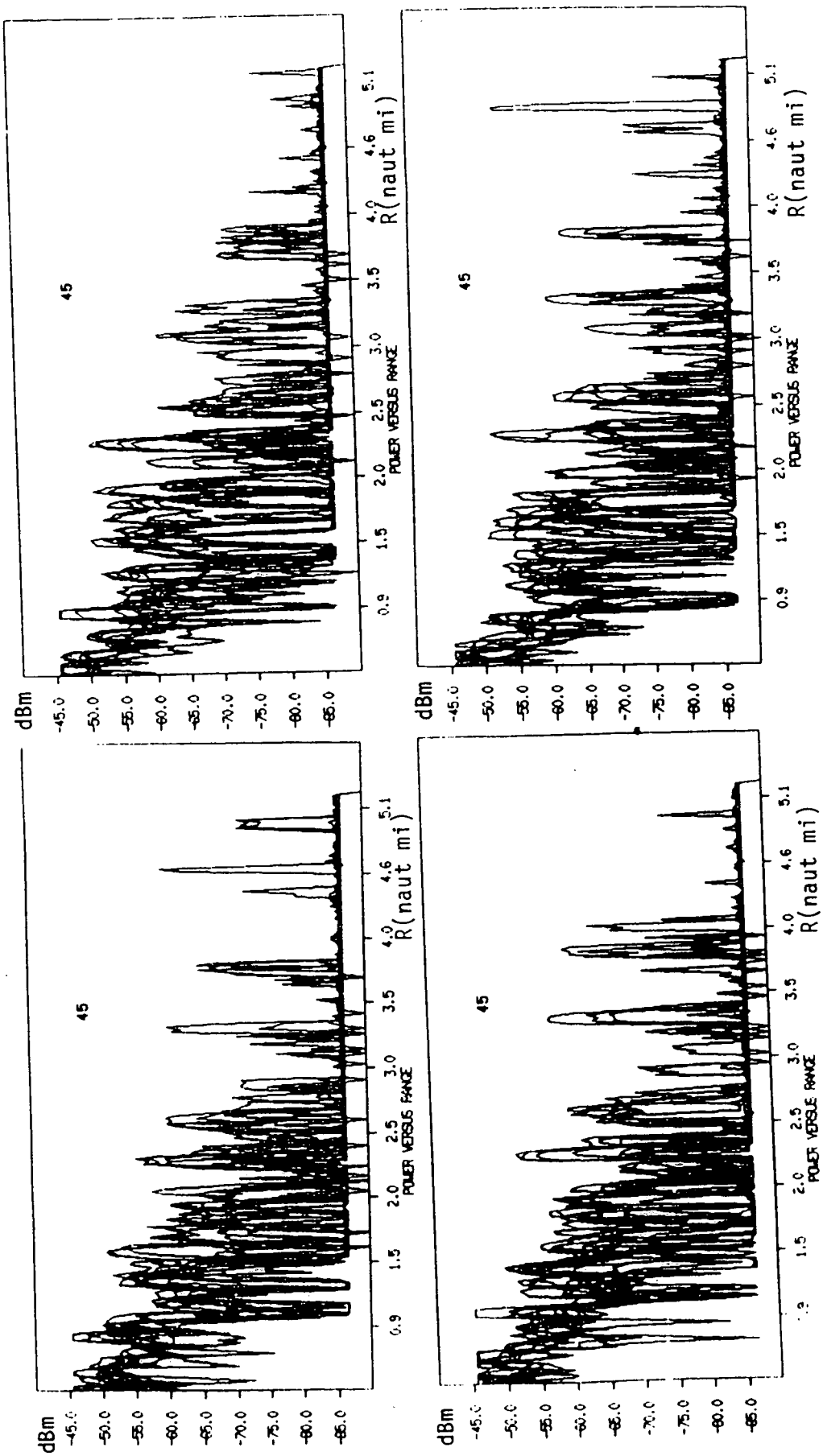

Figure 4.19 Received power data for berg 013, raw data, no averaging, scans 13 - 16.

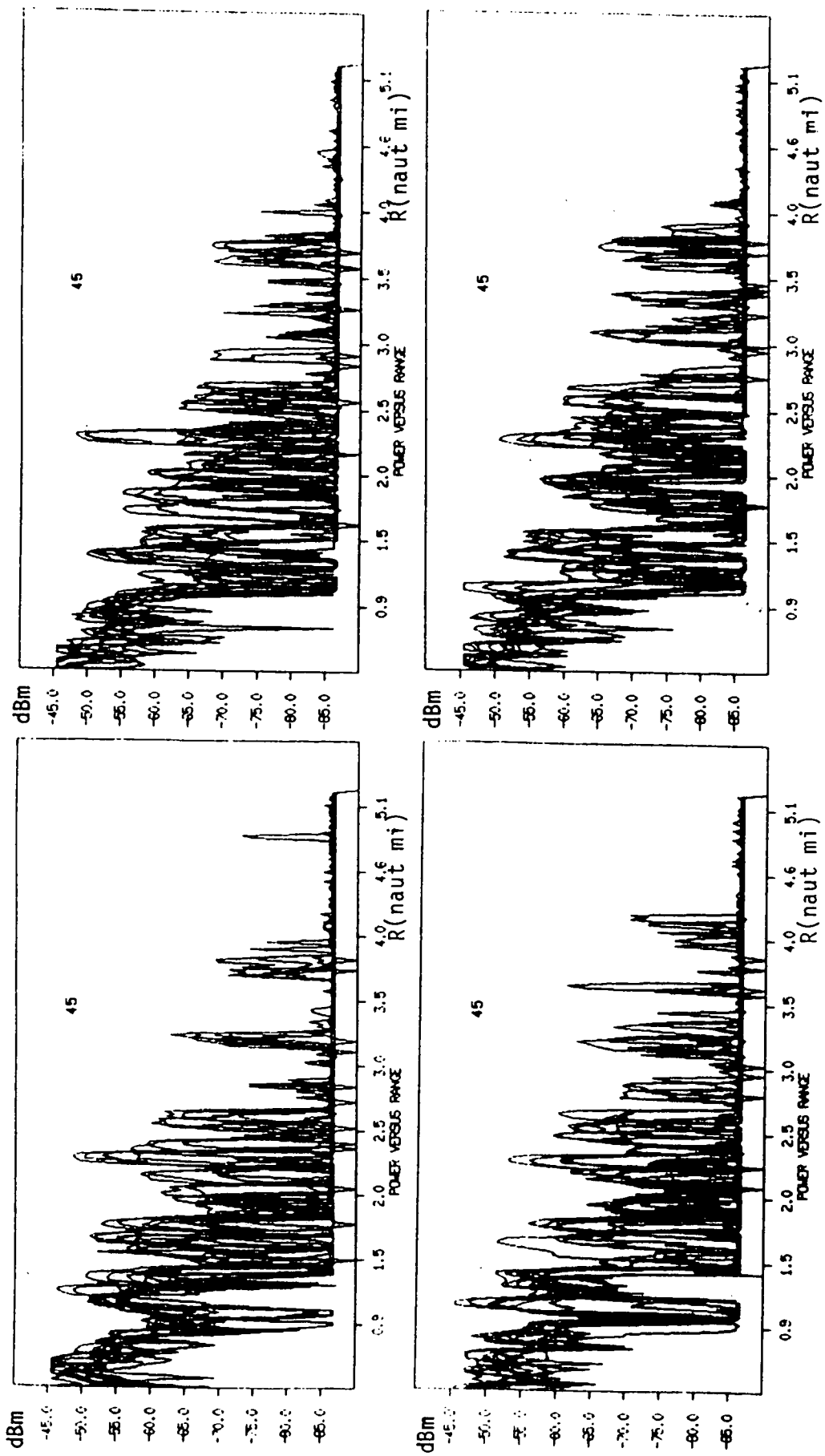

Figure 4.20 Received power data for berg 013, raw data, no averaging, scans 17 - 20.

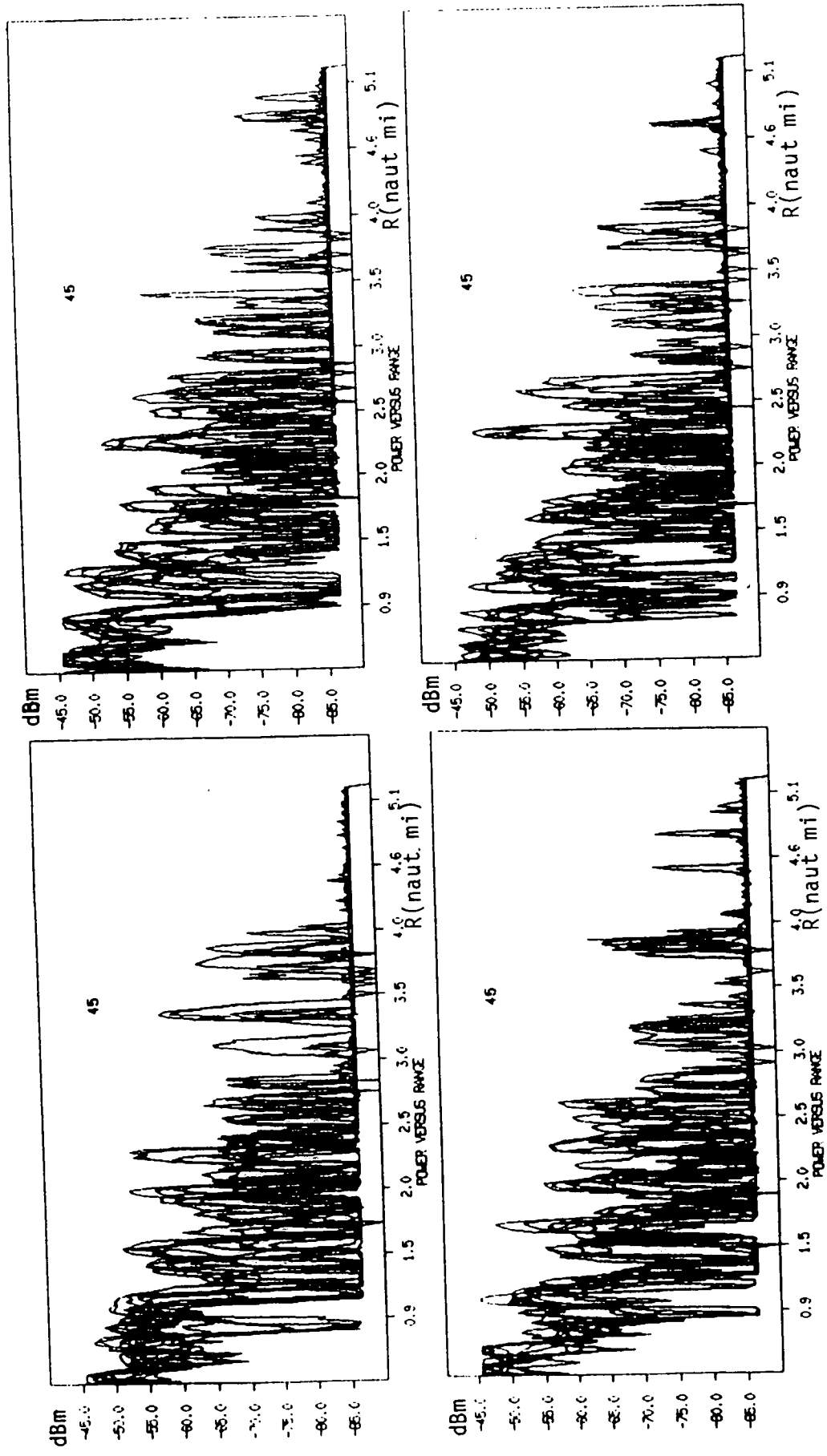

Figure 4.21 Received power data for berg 013, raw data, no averaging, scans 21 - 24.

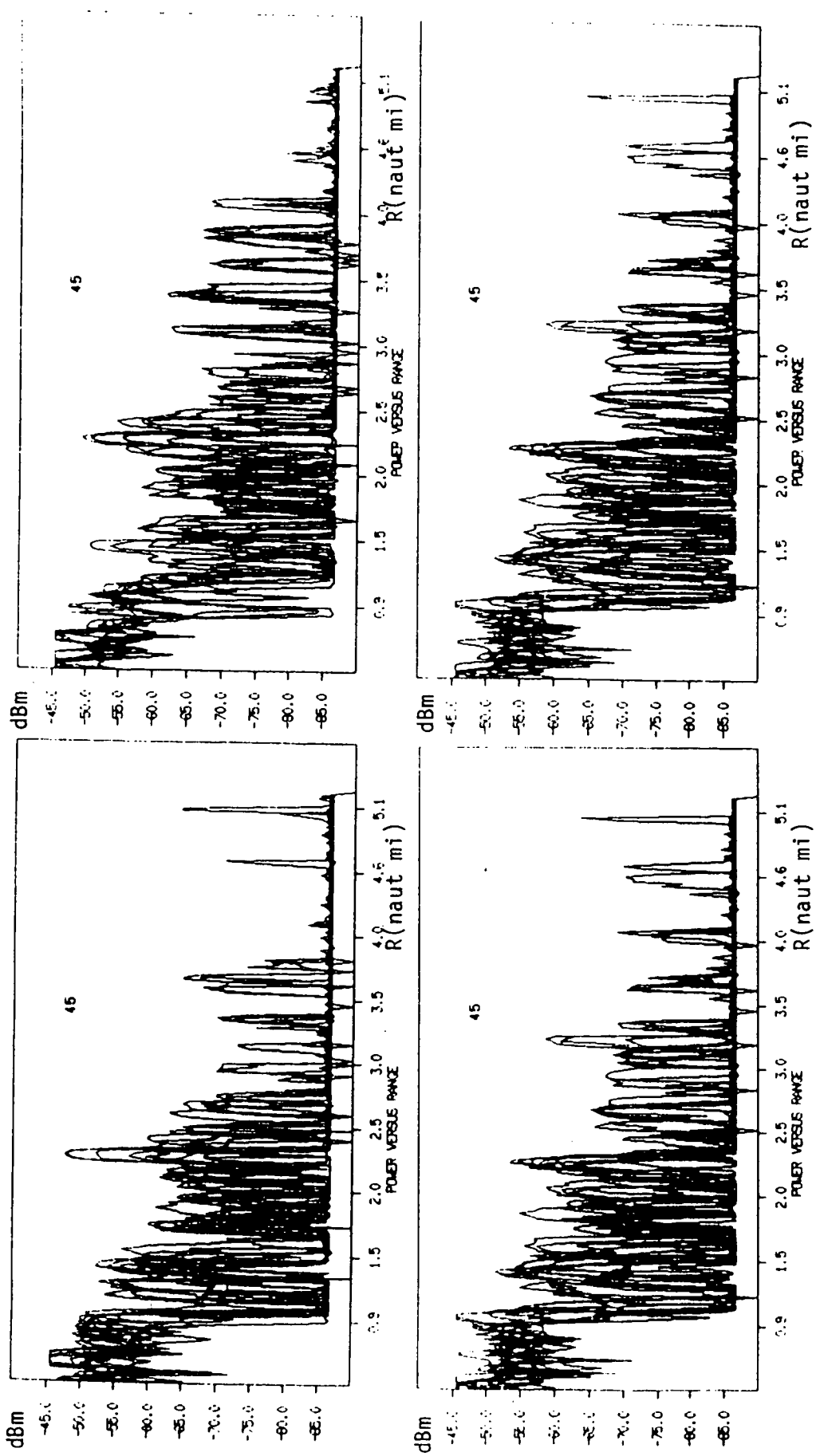

Figure 4.22 Received power data for berg 013, raw data, no averaging, scans 25 - 28.

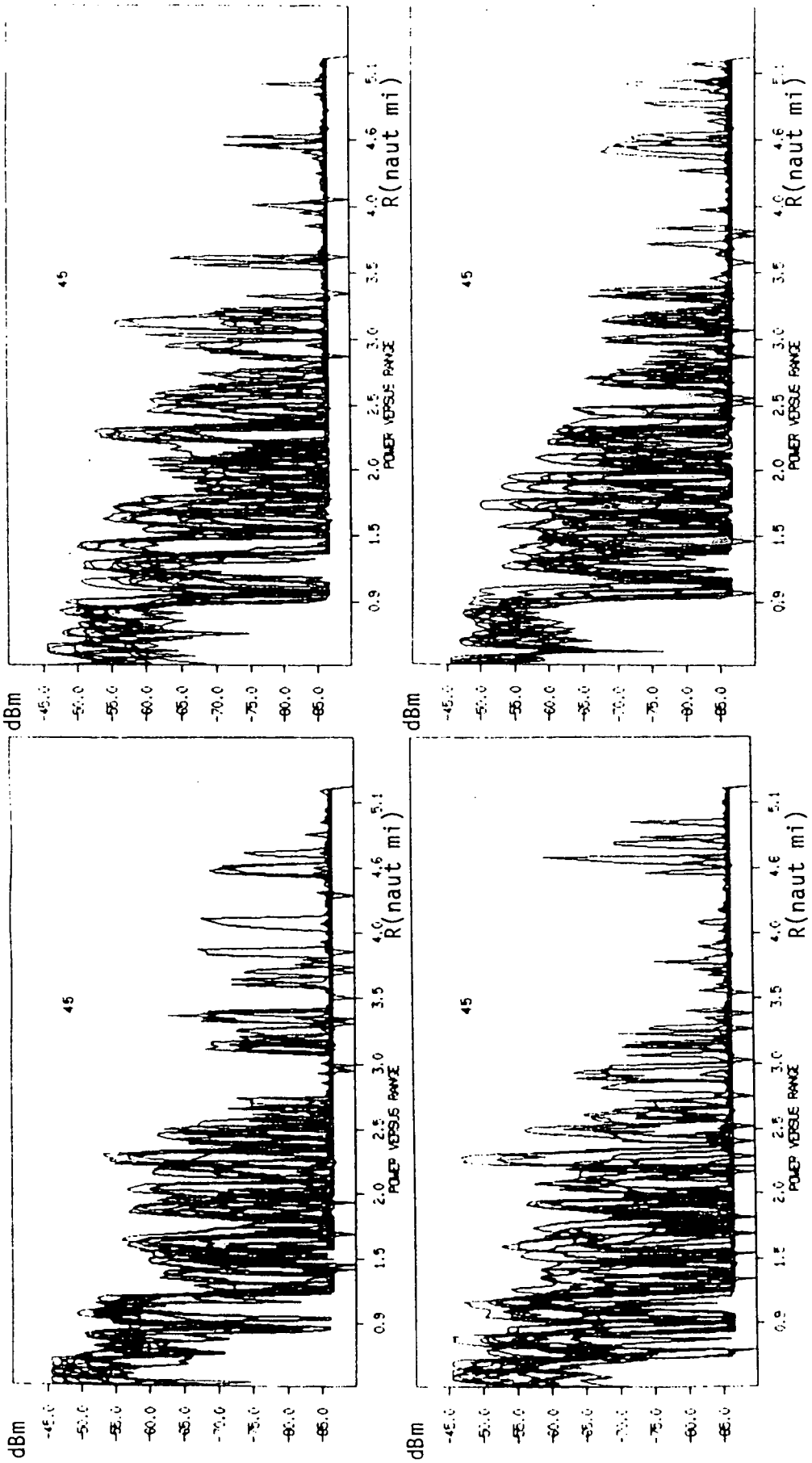

Figure 4.23 Received power data for berg 013, raw data, no averaging, scans 29 - 32.

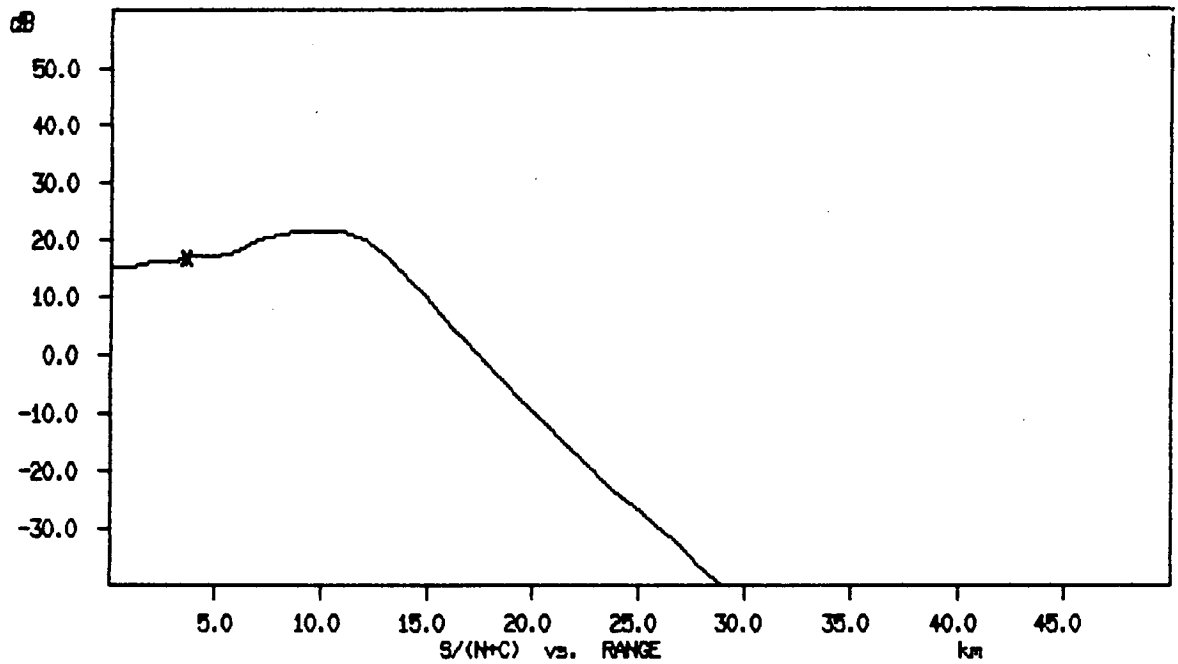

Figure 4.24: Model signal-to-clutter ratio for berg 013 in 3 m significant wave height and 13-kt wind (target at 4.3 km/2.3 naut mi).

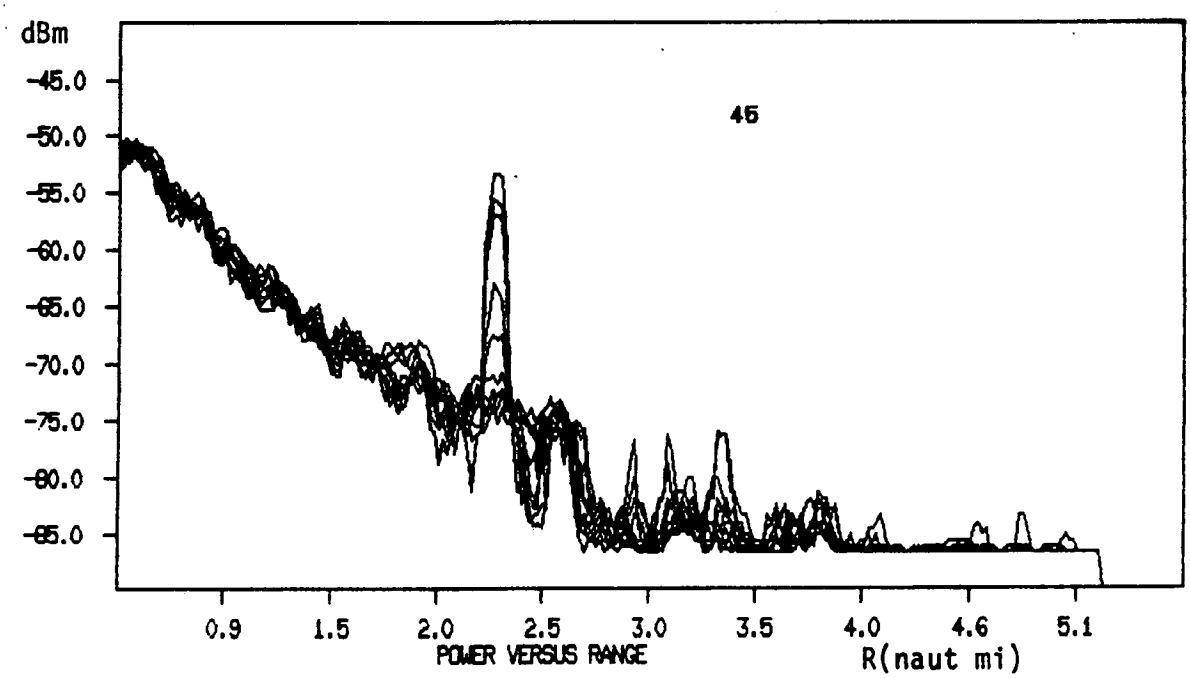

Figure 4.25: Received power data for berg 013 averaged over 32 scans.

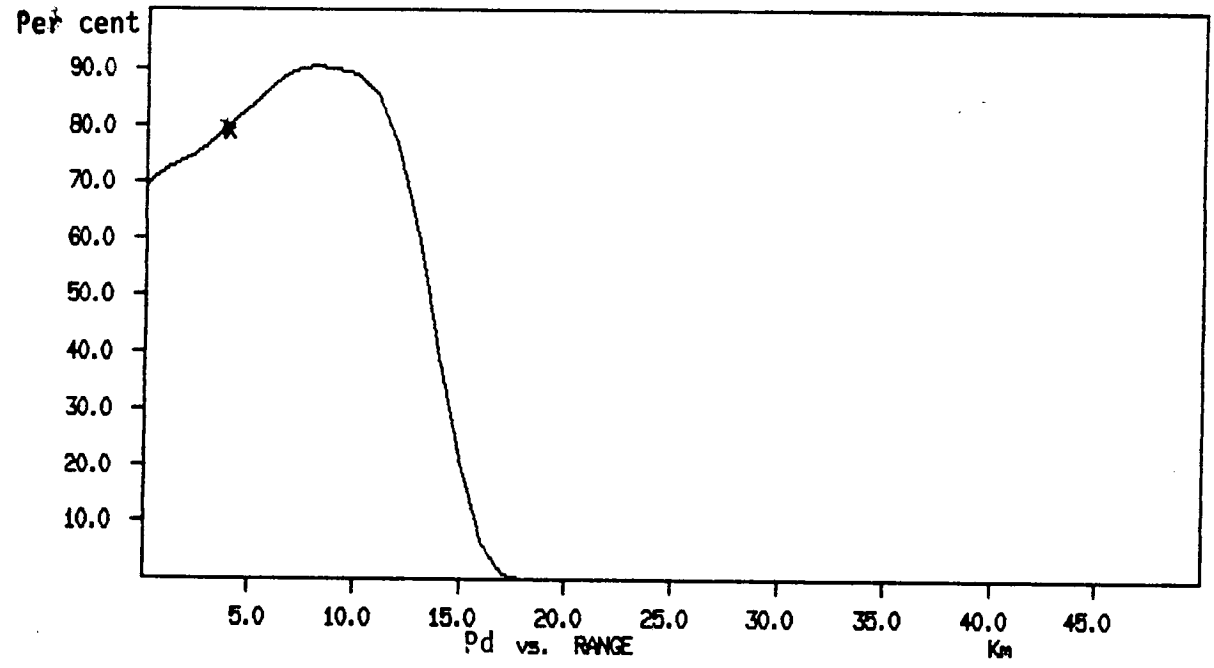

Figure 4.26. Model probability of detection for S/C of Figure 4.24. Pfa = 10^{-4}. Single-pulse detection.

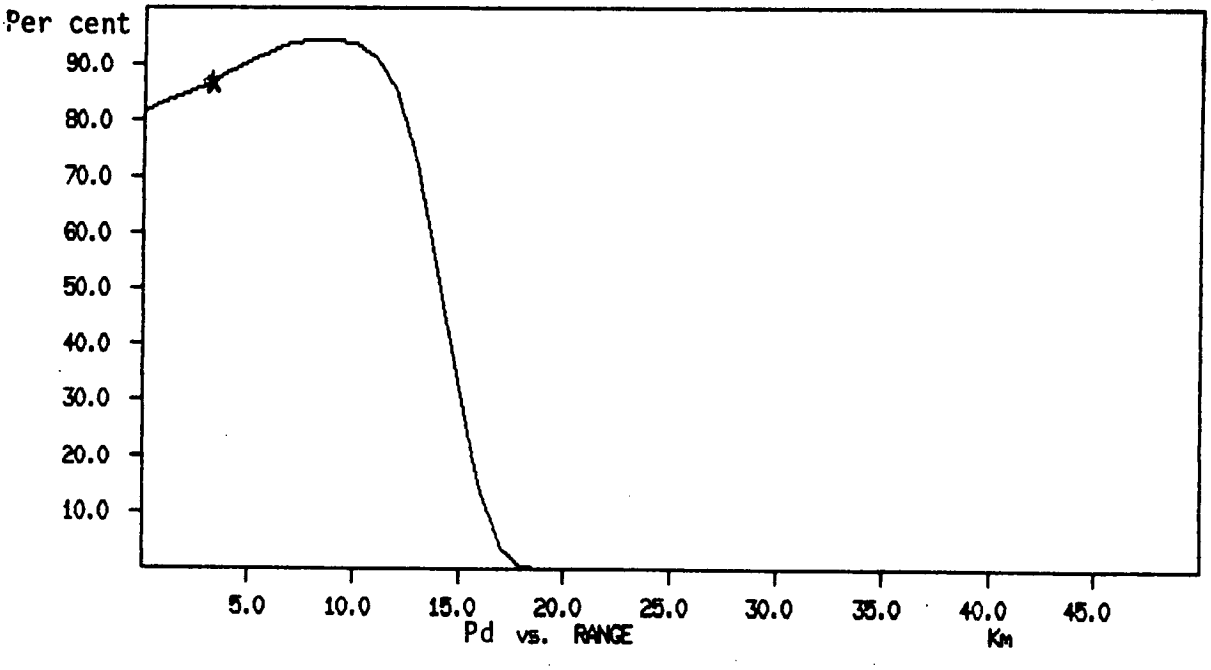

Figure 4.27: Model probability of detection for bergy bit 013 using a measured radar cross-section. Pfa = 10^{-4}. Single-pulse-detection.

4.4.2 Scan-to-Scan Averaging

The previous section has demonstrated the way in which computer models may be used to provide estimates of radar performance. This section demonstrates how scan-to-scan averaging can improve the capability.

An estimate of the improvement in the effective signal to clutter ratio by scan-to-scan averaging is easily obtained from the present data set. Using the previous example of the SDM in sea clutter, Figures 4.28 through 4.33 demonstrate the effect of averaging from 2 to 32 scans of the data from Berg 013. The improvement in the effective signal-to-clutter ratio is about 7-8 dB, agreeing well with the 10 log $\sqrt{n}$ theoretical value. It is difficult, however, to quantify the improvement in Pd. If we assume that the Pfa is 10^{-4}, as was done previously, then the Pd for the average of 32 scans is about 90%. The detection models assume a Gaussian-distributed noise and clearly as soon as we start to average the data the distribution changes, becoming narrower and more Gaussian. The effect in the blip-to-scan analysis will be to permit a lower threshold for the same probability of false alarm. This will increase the blip-to-scan ratio and, therefore, will improve probability of detection. The effect in the signal-to-clutter ratio analysis is not quite as clear, as probability of false alarm is not easily measured.

The following section presents the results of a detailed analysis on a SDD in sea clutter. The iceberg was target Berg 012 with a height 6 m, length 35 m, and width 48 m. The significant wave height was 3 m and the windspeed was 13-kt (the data were collected at the same time as those for Berg 013). The blip-to-scan analysis consisted of first performing the analysis for all 32 scans using the same threshold as was given in Figure 4.15. The data were then averaged into groups of two, a new threshold was set to keep the pfa constant and the blip-to-scan measurements made on the 16 groups of two. This procedure was repeated for up to eight groups of four scans averaged. The results are presented in Table 4.3., which indicates that by setting a proper threshold the Pd may be increased from 60% to 100% by averaging only four radar scans while keeping the Pfa constant. Increasing the threshold will have the effect of decreasing both the Pd and Pfa. Histograms for the power received from the iceberg, clutter and iceberg plus clutter are given in Figures 4.34 to 4.36 in which the thresholds used for each blip to scan measurement are indicated (i.e., 4 indicates threshold for four scans averaged). A well-defined clutter distribution may be seen in Figure 4.35 with a mean of about -70 dB. As more scans are averaged the distributions for clutter and iceberg will narrow and the threshold may be lowered to just above the mean clutter level. This situation will maintain false alarm rate while a maximizing probability of detection.

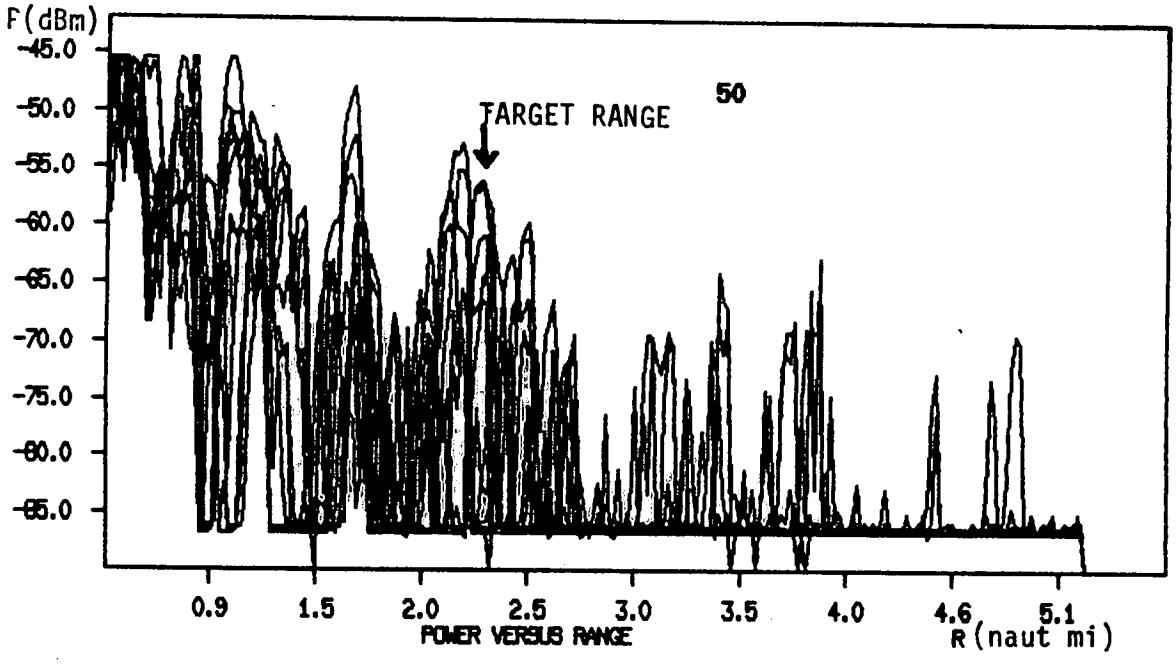

Figure 4.28: Single scan of radar data for a SDM in sea clutter (X-band).

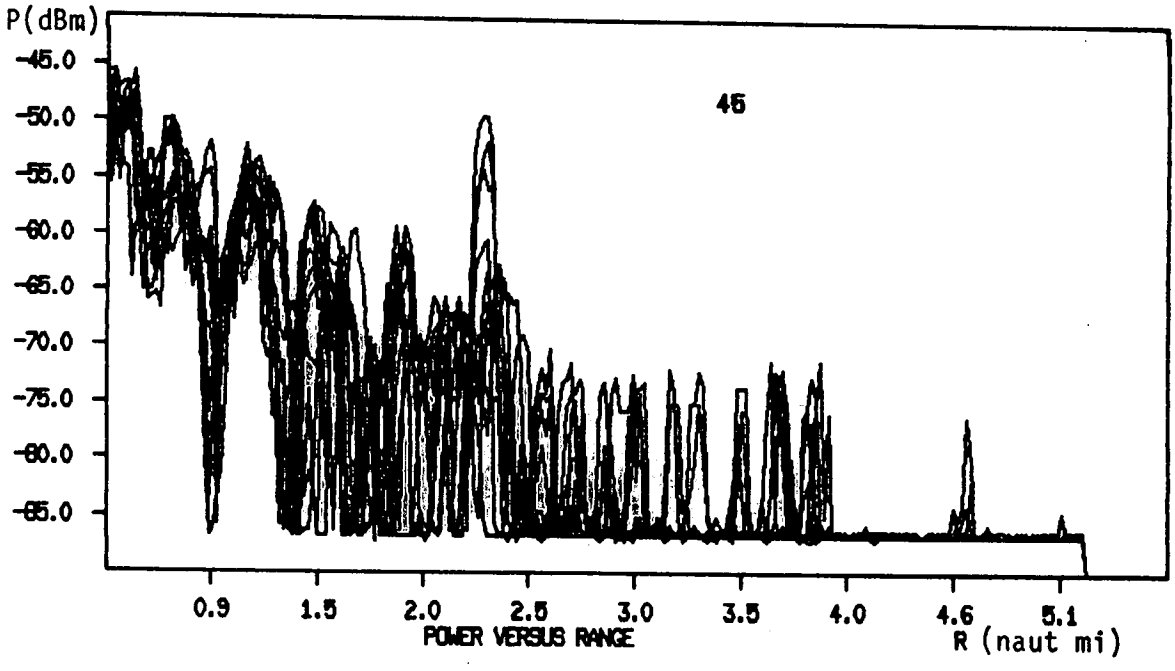

Figure 4.29: Average of two scans: SDM in sea clutter (X-band).

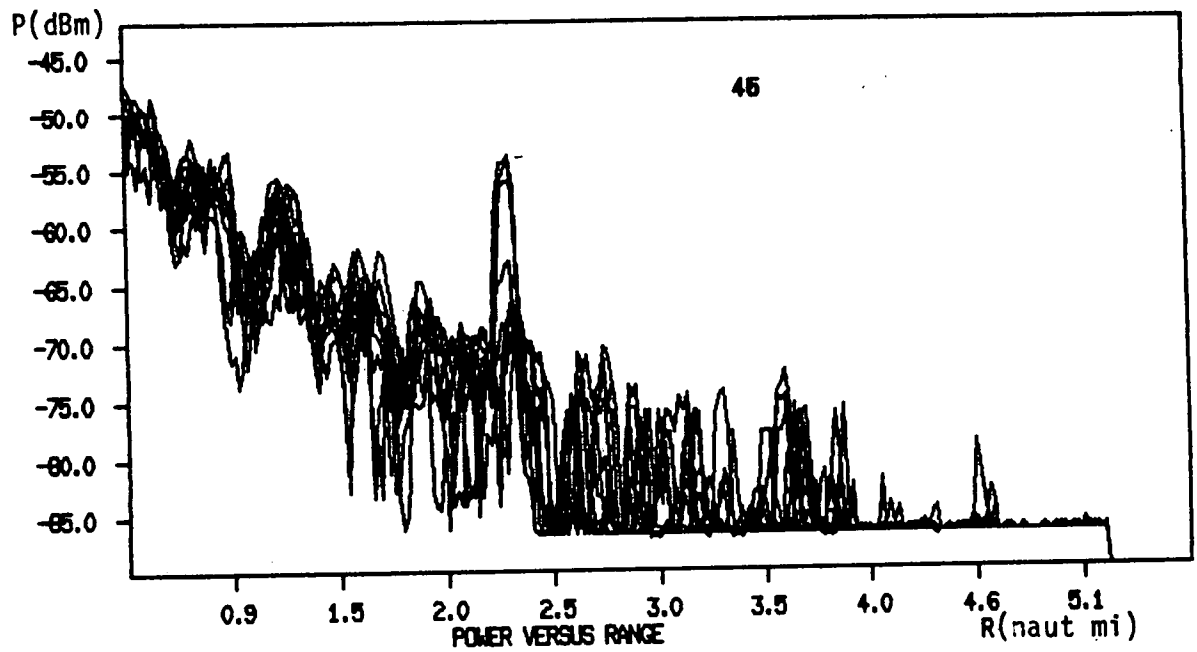

Figure 4.30: Average of four scans: SDM in sea clutter (X-band).

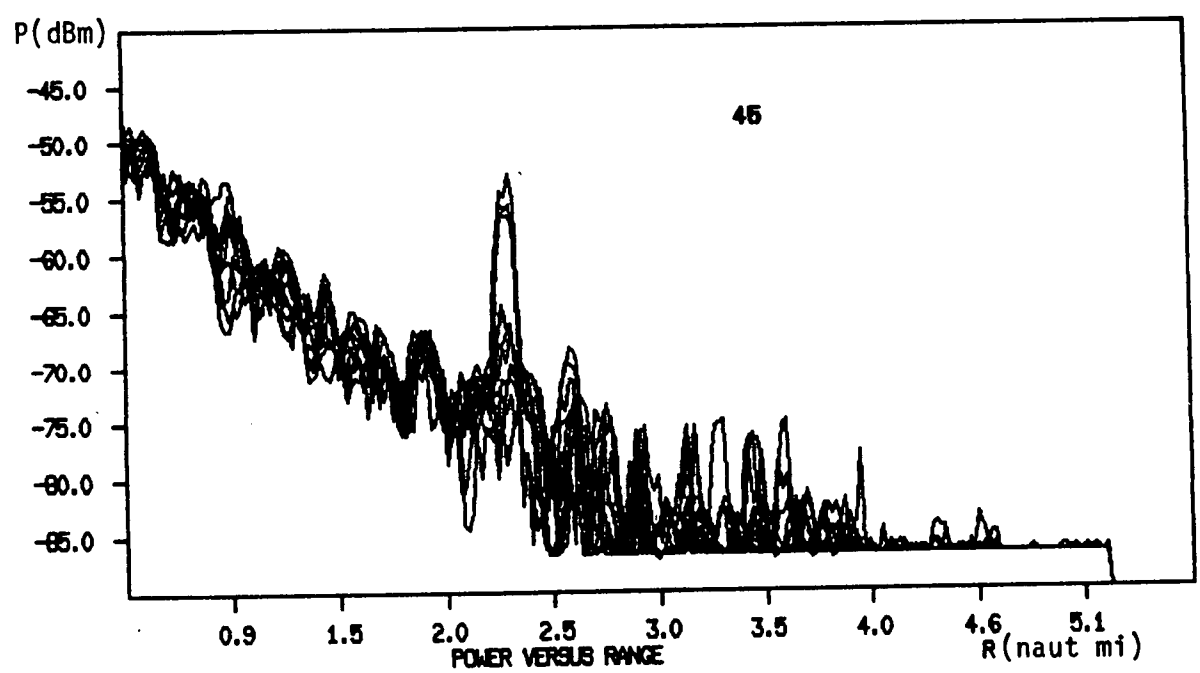

Figure 4.31: Average of eight scans: SDM in sea clutter (X-band).

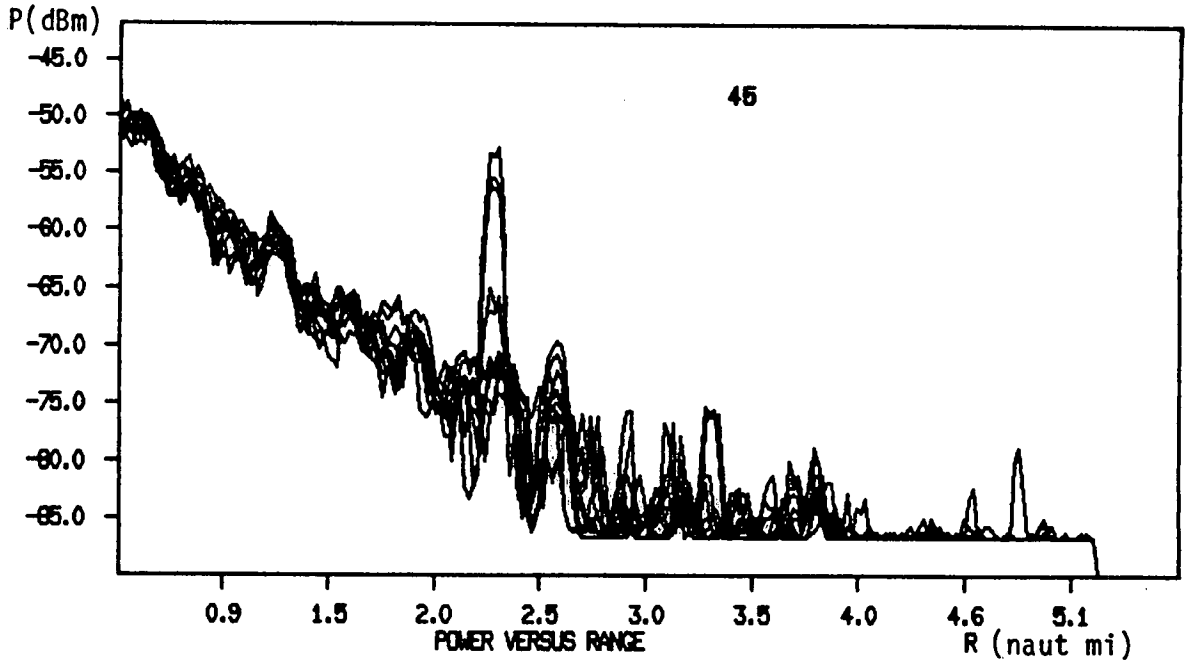

Figure 4.32: Average of 16 scans: SDM in sea clutter (X-band).

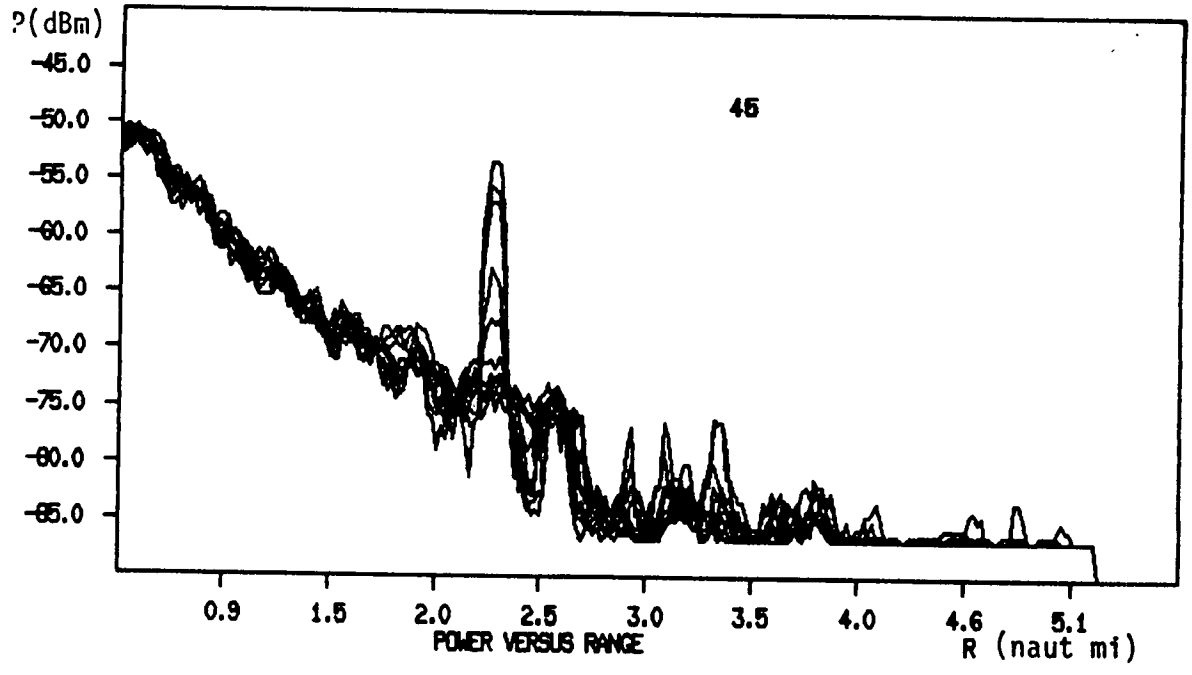

Figure 4.33: Average of 32 scans: SDM in sea clutter (X-band).

TABLE 4.3
Effect of scan-to scan averaging on probability of detection of a SDD (Berg 012) in sea clutter.

Number of scans averaged	Pd	Pfa	Threshold (dBm)
0	0.59	2×10^{-4}	- 51
2	0.9	1.6×10^{-4}	- 53
3	0.9	0.4×10^{-4}	- 55
4	1.0	2×10^{-4}	- 59

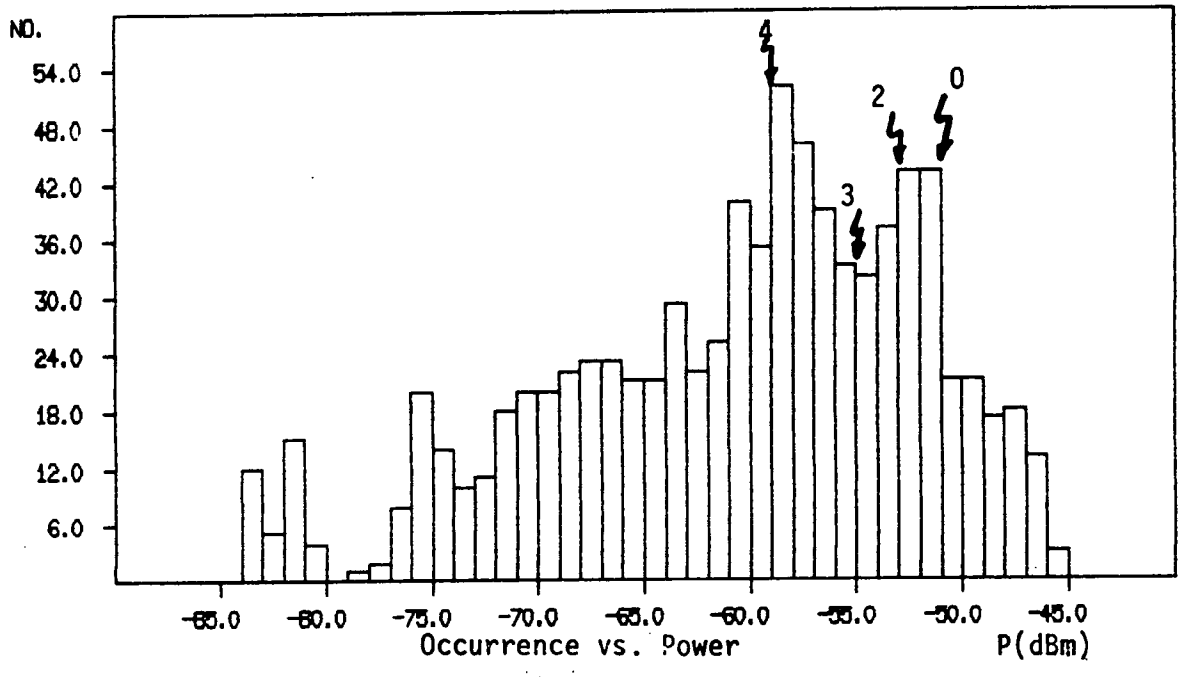

Figure 4.34: Histogram of received power from an SDD at X-band indicating four threshold levels used in a blip-to-scan analysis (Range = 2.0 naut mi).

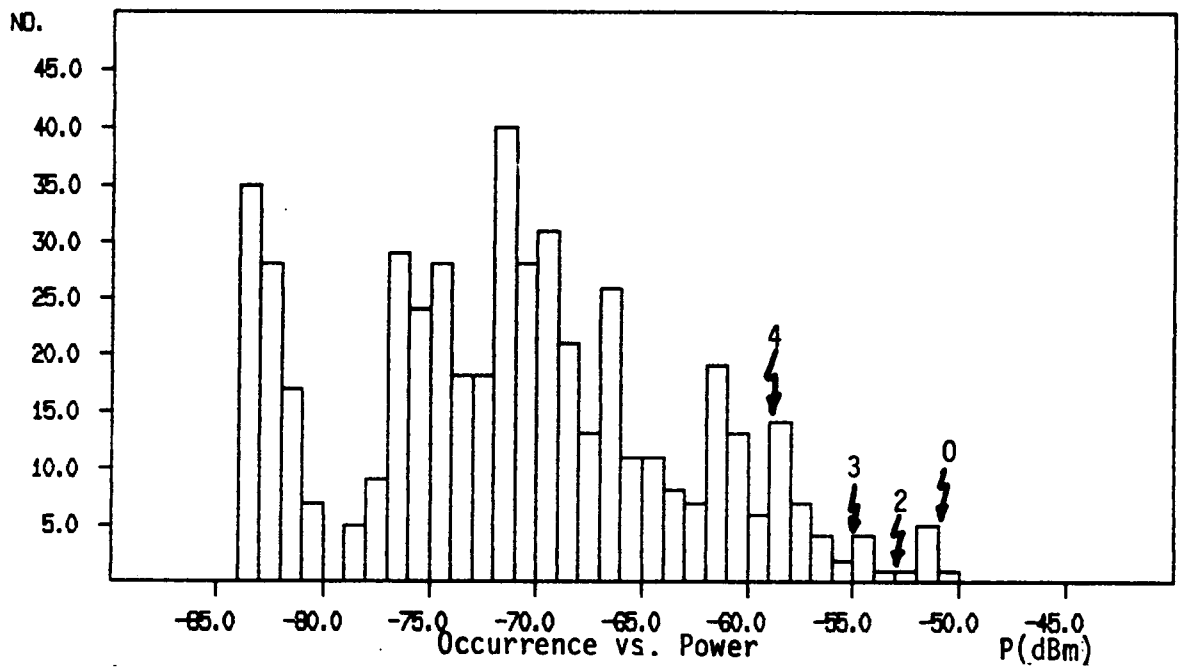

Figure 4.35: Histogram of received power from sea clutter at X-band indicating four thresholds used in a blip-to-scan analysis (Range = 2.0 naut mi). The clutter is taken from five consecutive range cells adjacent to the SDD of Figure 4.34.

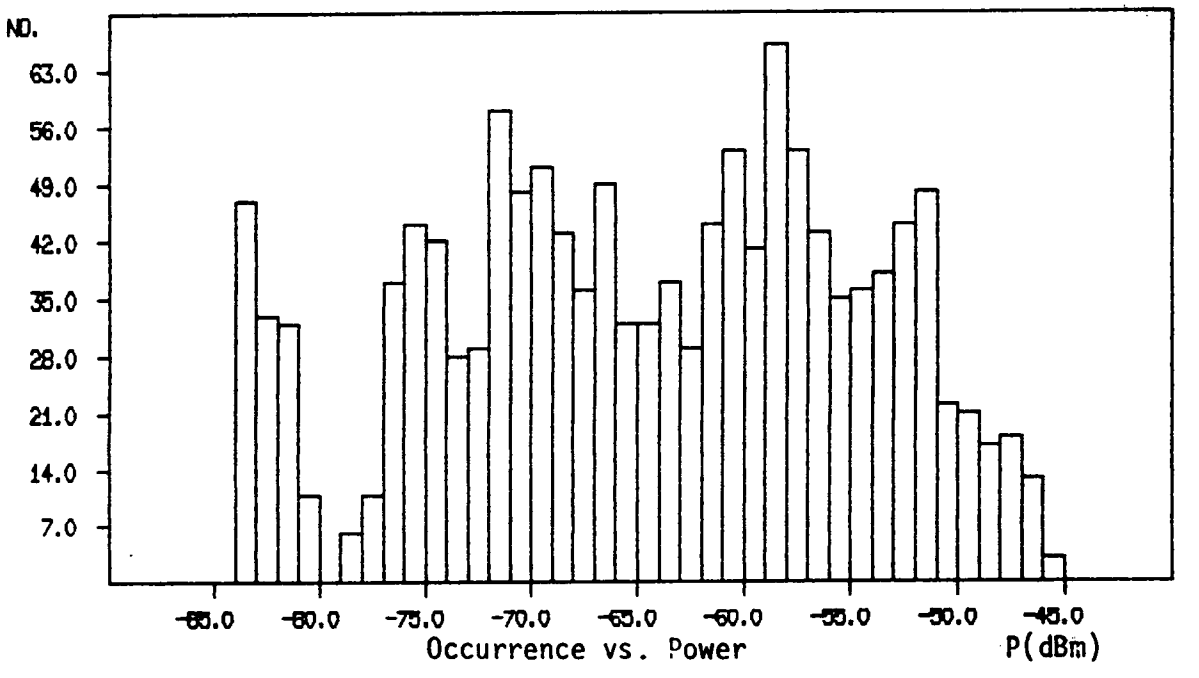

Figure 4.36: Histogram of received power from an SDD and sea clutter at X-band.

5.0 OPERATIONAL CONSIDERATIONS

The major effort of this study has been centred upon a quantitative assessment of iceberg detectability. The results of this work enable one to compare the technical capabilities of different systems under different environmental scenarios.

However, it is important to consider also the operational environment, and those factors that may enhance or detract from system capability. such as vessel motion, relative sophistication of the radar display, and operational tracking methodology. These factors are reviewed and a number of rule-of-thumb recommendations are made.

5.1 RADAR DISPLAY

The Racal-Decca Automatic Radar Plotting Aid (ARPA) was used during the field trial. A number of features are included in the system that improve an operator's ability to detect, classify, and track icebergs. A number of features are also present that have little application to the problem of iceberg management.

Racal-Decca claims that the most significant feature of the their ARPA design is the ability of the system to optimize the gain for each tracked target separately regardless of gain, rain clutter, or sea clutter settings in use by the operator. The "Clearscan" video-processing circuits reduce the sensitivity at all ranges and bearings where clutter exists. Racal-Decca also claims that this is done only to the extent that the auto-extraction system is able to discriminate wanted targets through clutter and interference. It is difficult to visualize how the system can discriminate these targets unless the target strength is greater than the clutter power. Therefore, it is unlikely that this expensive processing capability is of any use to the iceberg observer attempting to locate small targets buried in the clutter. Indeed it may be a hindrance, which is is supported by observation of small targets in clutter on the relatively simple Decca RM1210 also installed aboard the MV Polar Circle, when they were indistinguishable on the ARPA. In this case, for the detection of small targets in clutter, the height advantage of this smaller unit would be of no benefit, and would even be a hindrance.

On the other hand, for long-range detection of large targets, the processing features might enable the ARPA to outperform conventional displays. Even in this situation, however, the higher X-band ship's radar proved superior to the ARPA X- and S-band systems.

The principal advantage of the ARPA was its ability to track targets automatically once they had been detected. This feature was extremely useful in identifying icebergs through the automatic calculation of velocity. Invariably the icebergs would be moving at a constant velocity of between 1 and 2-kt. The associated numerical readout of speed, range, bearing, closest point of approach (CPA) and time to CPA, are helpful. Track history is useful in the Grand Banks area to assist in classifying fishing vessels and survey vessels.

Presentation of a video map although not used during the project could be useful for identifying drill-rig or platform positions, or the location of loading platforms and buoys.

The options for trial manoeuvres were of no use in the iceberg scenario.

In summary, the use of the "clearscan" processing is questionable for the detection of icebergs, especially for small icebergs at short range. The target-tracking capabilities are useful but probably do not alone justify the high cost of the equipment.

5.2 REAL-TIME DIGITAL DISPLAYS

The selection of the Racal-Decca ARPA has been an attempt to improve the detectability of icebergs. Although the apparent improvement is marginal at best, it does provide some useful functions to the operator. It also raises the question as to what system improvements might be attempted to improve iceberg detectability substantially. From a technical point of view, a number of image and signal-processing techniques have been recommended. These techniques can be implemented in true digital displays, of which the Racal-Decca ARPA cannot claim to be one. These techniques must be conducted in near real-time for them to be accepted by the operator, and, thus, most systems in existence cannot claim to satisfy this requirement. The implementation of a number of these techniques have been discussed in section 4 and in other reports, and techniques such as scan-to-scan averaging have been widely recommended. More advanced systems than the Racal-Decca ARPA are now commercially available. For example, the Computing Devices Company system known as SHINPADS (Shipboard Integrated Plotting and Display System) is a true digital display that can perform real-time processing. Scan-to-scan averaging is advertised as one of its strong points. Its drawback is the 4-bit quantitization of the signal, which restricts the potential of the system. As explained in Ryan et.al. (1985) it appears as if 8-bit quantitization is desirable. The SHINPAD system may have no difficulty in improving the signal strength of a large target, such as a ship, that is not embedded in

noise, but smaller targets hidden in clutter, or noise, will be harder to extract using a 4-bit system rather than an 8-bit system. There is a trade-off in memory requirements and data storage requirements, but the ultimate solution to the iceberg detection problem will require a capability to digitize, scan convert, process, and display 8-bit data in near real-time. This configuration is believed to be the system that will satisfy operator requirements in the iceberg environment. A true digital display with a capability of averaging and displaying 32 radar radials on the same bearing will also enable an automatic, or operator-selectable, dynamic-threshold processing capability to be implemented.

This ability will enable a maximum amount of noise and clutter to be presented at the threshold. By using the result of up to 32 or more averaged scans, a reasonable estimation of noise and clutter power can be made, and targets will not accidentally be thresholded out of the display as might be the case in a memory-less CFAR (constant false alarm rate) circuit, which effectively threshold the noise and clutter of one scan or less. Harvey and Ryan (1984) illustrate the results of this process.

To enable the highest resolution data to be displayed in near real-time, compromises such as B-scan displays or windowed displays might be acceptable. These will need to be evaluated in operational scenarios, but would likely meet with little resistance in an environment where trained operators are using the equipment, and where conventional marine radars are operating in parallel.

5.3 USE OF A RADAR PROPAGATION MODEL

A radar model of received signal strength from an iceberg must take into account the characteristics of the iceberg, the propagation path between the iceberg and the radar, the prevailing environmental conditions, and the radar parameters themselves. In addition, to provide an estimate of the detectability of the iceberg, it is necessary to model the competing signals such as sea clutter, rain clutter, and receiver noise. Expressions for the probability of detection may be incorporated into a computer model.

As part of this study, the authors have been asked to comment upon the fitted radars with the aim of making general recommendations as to the specifying operating guidelines for different situations. The aim, again is to maximize the operators probability of detection. Presumably, a small table could be produced that all operators would use to select radar-operating modes in different situations. After a month of observation of icebergs in many situations, it is difficult to determine an optimum operating mode. At best, it can be said that

S-band radar usually gives superior target detection capability (see section 4). It is not certain whether this effect results from superior S/N ratios, or, from visual perception differences caused by "clumpier" noise and clutter products on a radar display, which makes visual identification of targets easier. From an operator's point of view, height of antenna plays the most important part and improving detectability seems to be proportional to height in all conditions.

However, a solution to this problem of determining optimum operating modes may be possible. In a certain operational situation, on board a drilling rig, for example, an operator has a fixed set of equipment with which to work. By using an operational version of the model, with a menu-driven presentation, the operator could input propagation conditions, and, for certain basic iceberg types and sizes, preprogrammed if necessary, the model could recommend which radar and operating mode would provide the best probability of detection. STC (sensitivity time control) and gain settings could be included to provide the operator with recommendations to optimize the system's performance.

5.4 OPERATIONAL TECHNIQUES

A number of generalizations can be made concerning the technique used by an observer to detect icebergs.

First, continuous observation of a radar PPI (plan position indicator) is not necessary. Given the slow movement of icebergs and tracking ships, or the fact that a drilling platform is stationary, observations every 15 min. of 30-60 scans would appear to be acceptable. For long-range detection of large icebergs from a stationary platform, observations once an hour would be acceptable.

Secondly, the range of target fading or appearance is generally from 0.5 to 2 naut mi depending on conditions, obviating the need for continuous observation. Once detected, operators should use an auto-tracking function, however, great care must be taken not to attempt to track small icebergs in sea clutter automatically as existing systems are not capable of providing reliable tracking under these conditions. Target plots need not be updated more than twice per hour.

Thirdly, automatic alarms are of dubious value, detecting only the largest icebergs with any confidence. Range settings for normal operations should be positioned at 12 naut mi range. During heavy precipitation or in heavy seas the appropriate range setting should be 6 naut mi when looking for bergy bits, growlers, or small icebergs. Periodically the range should be extended out to 24 naut mi for large icebergs. Under the conditions, an operator should increase the gain for small target detection and should watch the radar continuously.

5.5 VESSEL MOTION

Much discussion by critics of ship-borne experiments has led to the belief that use of a motion-prone platform would invariably lead to an inferior data set. However, qualitative observations of both data as they were being recorded and comparison of consecutive scans of recorded data have shown that platform motion plays little part in determining the variability of the data. First, rolling can be almost eliminated by selection of a course parallel to wave or swell direction. Secondly, pitching effects can be minimized by steaming downsea. These two steps would almost certainly ensure that signal returns fall within the half-power limits of the antenna's vertical beamwidth. This effect has been further investigated under a contract issued by the Department of Fisheries and Oceans to investigate the time variation of radar returns in a number of different situations using the ESRF data.

Thirdly, in the case of small icebergs, the signal variability will be much more dependant upon the physical cross-section of the iceberg as viewed by the radar in higher sea states. This view can range from nothing, when the iceberg is hidden by waves or swell, to a maximum when salt-water spray is forced high into the air after striking the iceberg.

5.6 OPERATIONAL DETECTION RANGES

Continuous visual observation of the radar displays enabled the ranges of target acquisition to be compiled. Table 5.1 identifies the detection ranges for most of the icebergs that were recorded. Note that in several cases the ship's radar was the first to detect a target. Detection was generally considered to occur when two successive blips in one spot occurred during two successive scans. At this point, the range was recorded and if subsequently the target disappeared, then it was considered to be a false alarm. If the target disappeared for a few scans and reappeared, then the initial detection was considered valid.

Figure 5.1 illustrates the approximate area of radar cross-section as a function of detection range. The curve should be used only as a guide, as detection range will vary depending upon prevailing conditions. However, in general, all icebergs with an average cross-section of greater 100 m^2 in area will be detected at a range of 4 naut mi or more. Also, icebergs with a cross-section of 1,000 m^2 will be detected at a range of 8 naut mi or more. This rule-of-thumb is applicable to radars with an antenna height of about 15 m, or the height usually encountered on workboats. These ranges are less than those given by Budinger (1960), however, his figures were taken from studies performed aboard U.S. Coast Guard ships, presumably with much higher radar antennae.

TABLE 5.1
Detection ranges of icebergs

Iceberg Class.	Target I.D. (Berg)	Detection range (naut mi)	System	Comments
MDD	001 D	11.0 naut mi	-	
MPI	002	11.0 naut mi	-	Lost at 12.0 naut mi still visible by eye
BB	003	6.0 naut mi	-	
-	Susan R2	6.3 naut mi	Both	
MDD	001E	6.4 naut mi	-	Lost in clutter at 8.0 naut mi
-	004	-	-	
MPI	002B	11.1 naut mi	-	
LPI	005	17.26 naut mi	ARPA	
		18.0 naut mi	Ship's radar	
MWD	006	8.2 naut mi	-	Lost at 11.0 naut mi
LDD	007	8.0 naut mi	ARPA	
MPI	008	9.6 naut mi		
SWD	009	6.5 naut mi	SHIP	
		6.0 naut mi	ARPA S-band	
		6.5 naut mi	ARPA X-band	
SDD	012	6.0 naut mi		
SDM	013	6.6 naut mi	-	Lost at 5.6 naut mi
MWD	014	11.5 naut mi	-	
MBL	015	13.3 naut mi	-	
LDD	016	14.5 naut mi	-	
MBL	017	9.5 naut mi	-	Faded at 7.5 naut mi
LDM	019	8.1 naut mi	-	Faded at 10.5 naut mi Lost at 12.5 naut mi
MBL	020	9.5 naut mi	-	Lost at 12.0 naut mi
MBL	021	8.0 naut mi	-	
ICE	022	1.8 naut mi	-	Lost in clutter at 0.3 naut mi
-	023	13.2 naut mi	-	
MBL	050	10.0 naut mi	-	Lost at 10.5 naut mi
GRW	051	1.7 naut mi	ARPA	
STA	052	5.2 naut mi	-	Lost at 6.0 naut mi
SBL	053	5.9 naut mi	ARPA	Fades at 6.5 naut mi
			ARPA	Lost at 7.5 naut mi
			Ship's radar	Lost at 8.5 naut mi
BB	055	None	-	Visual detection at 4.0 naut mi

Table 5.1 continued ....

Iceberg Class.	Target I.D. (Berg)	Detection Range (naut mi)	System	Comments
LTA	056	5.8 naut mi	-	
-	057	12.3 naut mi	Ship's radar	
		11.4 naut mi	ARPA	
MBL	059	12.7 naut mi	-	
MWD	060	7.3 naut mi		Faded at 5.0 naut mi (X+S)
ICE	061-64	None	-	Visual detection 1.0 naut mi
ICE	065	2.5 naut mi	ARPA S-band	
SDM	066	5.0 naut mi	ARPA	
SBL	067	5.0 naut mi	ARPA	
MPI	068	13.0 naut mi	-	
MDM	069	9.6 naut mi	-	
GRW	070	0.4 naut mi	-	
ICE	072	1.7 naut mi	-	Maximum detection range 1.8 naut mi Redetected at 1.3 naut mi
BB	078	0.9 naut mi	-	
ICE	079	.25-.3 naut mi	-	Barely detectable
ICE	082	0.2 naut mi	-	Maximum detection range 0.45 naut mi

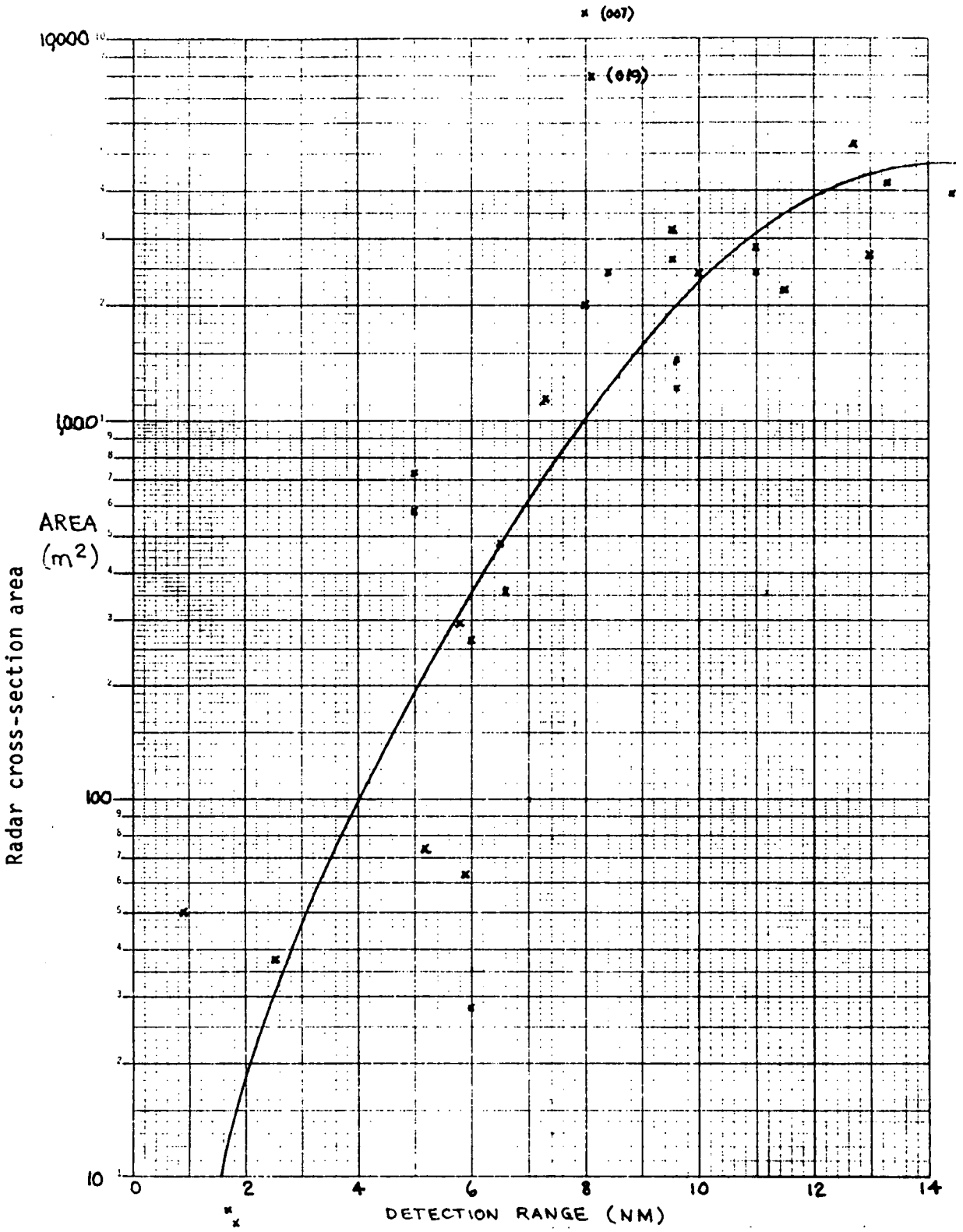

Figure 5.1: Radar cross-section area versus detection range for icebergs from a typical workboat with a 15-m antenna height.

Given that bergy bit detection is required, a workboat could steam the search pattern described in Figure 5.2 and would likely detect all bergy bits or larger icebergs in its sector. This assumes a 12-kt speed of advance, and a 1-kt iceberg velocity in any direction, as long as the long-term movement of the iceberg is within 60° of the sector axis. In this case one vessel on station could provide continuous surveillance around the drilling rig or production facility, and could give at least 12 hours notice for rig countermeasures to be taken. This coverage would be essentially the same as Flight Route Number Three outlined in the Grand Banks Operators Ice Management Plan (Mobil Oil Canada 1983), with the exception that alert times would be shorter. Increasing the alert times would narrow the sector coverage correspondingly. As depicted in Figure 5.2, the workboat would never be more than two hours from the rig.

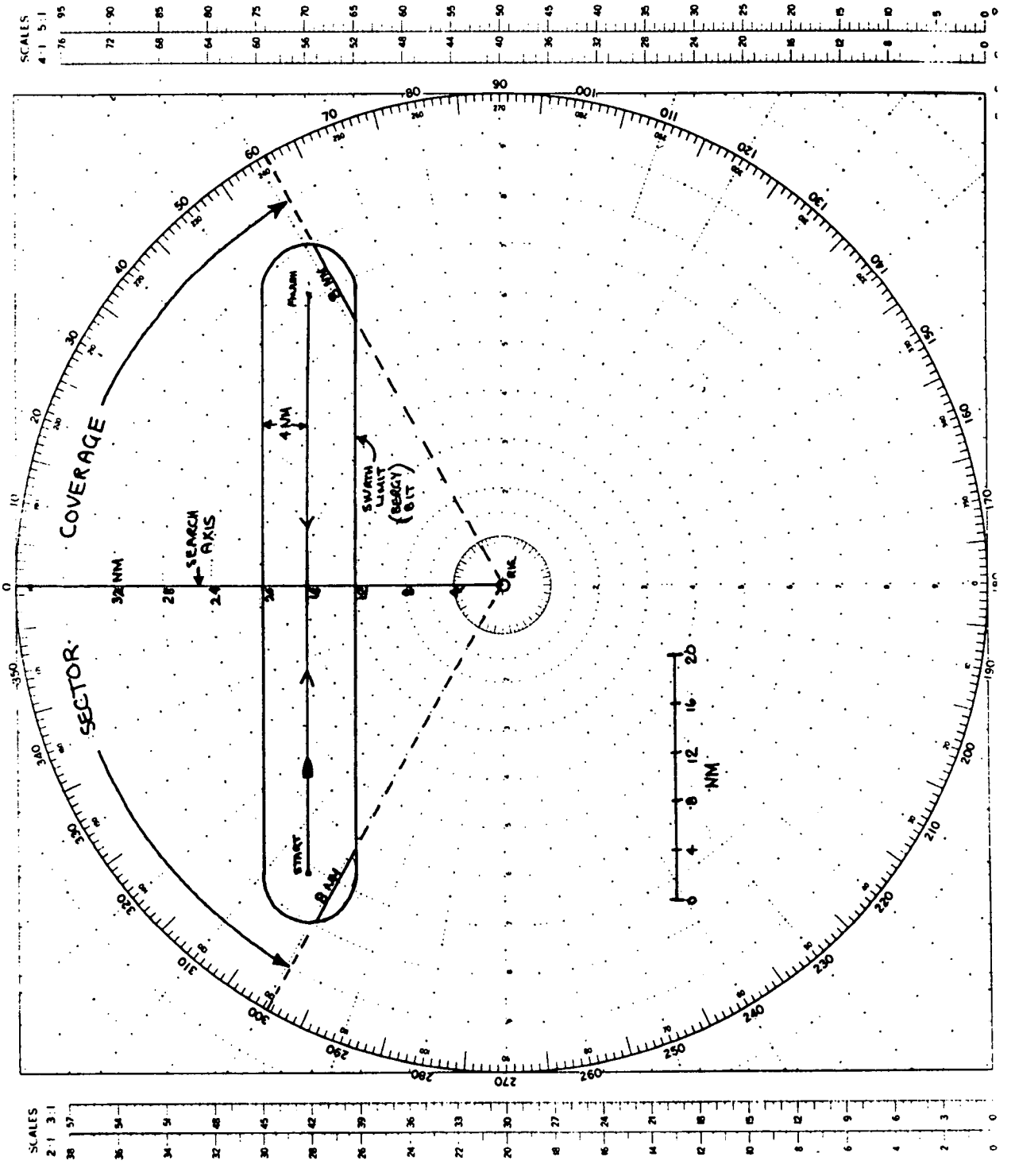

Figure 5.2: Plan view of workboat coverage for 100% bergy bit detection.

6.0 CONCLUSIONS

The major objective was to quantify the capability of marine radars to detect small ice targets. By using a ship instead of a fixed platform, a large data set was collected, which was complementary to that collected on board the SEDCO 706. Not only were more targets collected, but the data points were collected under different environmental operational conditions. The radar data were supported by superior target verification and are characterized by their higher resolution. The radar model, against which the data are generally compared, has been validated, and with the refinements and enhancement of the output, is now considered to be a reliable method of predicting iceberg detectability under most conditions.

6.1 SUMMARY OF GENERAL ACHIEVEMENTS

The data collection phase succeeded in the collection of large quantities of data for small and medium icebergs in different environmental conditions, specifically enabling the calculation of iceberg radar cross-sections. In addition, the meteorological parameters necessary to calculate evaporation duct parameters have been documented, although these data were not used to evaluate subrefraction and super-refraction conditions in the subsequent analysis. As a by-product of the analysis, data-processing techniques that were used pointed to a number of methods for improving signal-to-noise and signal-to-clutter ratios. Therefore, the requirements outlined as program priorities were achieved. These points also formed part of the recommendation for future work as outlined in Ryan et.al. (1985). The other major recommendation involved further investigation of data for the dependence of sea clutter on wind speed and direction and significant wave height which was also accomplished to a limited extent.

The three specific limitations of the data set collected during the program on board the SEDCO 706 were addressed. Large quantities of target data in sea clutter were collected. Although not exhaustive, the detailed analysis of a limited amount of sea clutter confirmed that the data are of sufficient quality to enable the direct comparison of ocean back-scatter coefficients with published values. In addition, the data will allow the extrapolation of present published results and contains information not previously documented concerning S-band radar cross-sections of icebergs. Lastly, enough data were collected and analysed that it is safe to say further analysis will allow comparisons of radar cross-sections of icebergs with their average cross-sectional area, if desired.

6.2 CONCLUSIONS

Sixty-eight targets containing 42 icebergs and 23 sea-ice targets were recorded. In addition, calibrated reference target data enabled the confirmation of system losses and antenna gains. Good agreement between the calibrated target data and theoretical values indicate that quantitative measurements of received power from the data is possible.

This enabled the influence of sea clutter to be quantified for significant wave height of 0.3-7 m and numerous wind speeds. Again, excellent agreement was apparent between X-band data and the data of Nathanson (1969). The dependence of X-band sea clutter on wind is minor in comparison to the effect of significant wave height. The Sittrop model shows best agreement in fully developed seas.

Preliminary analysis has indicated that S-band sea clutter is more variable for a given significant wave height which would lead one to believe that there is a greater dependence upon wind direction and swell direction than in the case of X-band radar.

Sufficient data were available to make quantitative measurements of radar cross-sections of icebergs. These values vary depending upon the orientation and behaviour of the iceberg. X-band radar cross-sections are up to 10 times larger than S-band radar cross-sections. The results agree closely with existing models for X-band. As no model currently exists to estimate iceberg cross-sections for S-band radars, the actual results seem reasonable.

The Viatec radar model has been used to calculate probability of detection for iceberg targets and compares favourably with a blip-to-scan technique used in the analysis. An improvement in the effective signal-to-noise ratio by 10 log $\sqrt{n}$ is demonstrated when n consecutive radar scans are averaged. By modifying the blip-to-scan analysis procedures, it is possible to quantify the improvement in probability of detection when scan-to-scan averaging is used. By setting the proper detection thresholds, the probability of detection in one case was improved by 40 per cent by averaging only 4 radar scans. This improvement points to a need to investigate the advantages of using scan-to-scan averaging combined with dynamic threshold processing.

6.3 OPERATIONAL RESULTS

The relatively sophisticated ARPA unit did not provide superior detection of icebergs. Antenna height appears to be the predominant factor in improving iceberg detectability in all conditions. The S-band radar generally was the preferable detection radar for icebergs.

The detection range for bergy bits from a ship similar to the MV Polar Circle is expected to be 4 naut mi, and small icebergs can be detected reliably at 8 naut mi.

7.0 RECOMMENDATIONS

It has been demonstrated during this study that significant performance improvements can be incorporated into standard marine radars by using signal-processing techniques to increase the probability of detection of icebergs. To be confident that the results of using different techniques are maximized, a number of areas require further investigation. It is not considered advisable, however, to collect any more non-coherent marine radar data in the Hibernia area. The quantity and quality of the data set collected during this program should satisfy researchers in the foreseeable future.

7.1 FUTURE STUDIES

A number of outstanding requirements for further work resulting from the 1984 field program have been met and the data set is now considered satisfactory to meet all of these requirements. However, because of the limited analysis that was carried out, further analysis is desirable which includes, but is not limited to, the following studies:

a) Further analysis is required to quantify the effects of wind and swell direction on sea clutter returns, particularly for S-band radar data. More investigation into the variability of S-band radar returns over time is advisable.

b) Further development of an S-band sea-clutter model should take into account wind speed and direction and wave and swell direction.

c) An iceberg cross-section model for S-band radar should be developed and compared with data collected.

d) The effects of ducting require evaluation. Because of the much lower antenna height on the vessel, as compared to those on board the SEDCO 706, a situation may exist whereby when ducting conditions are present, the ship's radar will always be under the duct ceiling, and will experience the effects of this phenomena phenomena, whereas a rig-based radar may not. In contrast with the 1984 program, super- and subrefraction effects, if present, did not seem to give unusual or variable detection ranges, except in a few cases.

7.2 SIGNAL PROCESSING

Given a certain radar system, aside from elevating the antenna, signal processing has been shown to provide the most significant improvements in target detectability. Further studies to quantify the effects of scan-to-scan processing are advisable, using the current data. Also, a manual or automatic threshold optimization for different filtering schemes improves detectability. These simple processing techniques may be implemented in real-time at a nominal cost. Statistical decision-making criteria should be evaluated for use with processed data, as an aid to target designation.

7.3 HARDWARE SPECIFICATION

It is recommended that from optimum iceberg detection relatively unsophisticated marine radars combined with purpose-built, signal-processing, and display systems be specified for future installation on board workboats, drilling rigs, and production facilities. Sophisticated target-plotting and display systems, such as those manufactured for commercial shipping, are not considered cost effective.

Future specifications should ensure that at least one radar antenna is mounted as high as possible.

8.0 REFERENCES

Blake, L.V. 1980. Radar range performance analysis. D.C. Heath and Company.

Budinger, T.F. 1960. Iceberg detection by radar. International Ice Patrol Bulletin No. 45, United States Coast Guard.

Dawe, B.R. 1985. A radar cross section model for icebergs. IEEE 1985 International Radar Conference, Arlington, Virginia, 6-9 May 1985.

Harvey, M.J. and Ryan, J.P. 1984. Radar digitization, conversion and analysis of an ice hazard detection/collision avoidance system. Transportation Development Centre Report TP6067E. Montreal.

Lowry, R.T., A. Stuart, J.B. Mercer, and J.R. Benoit. 1984. Modelling the radar detection of icebergs. Presented at the Ninth Canadian Symposium on Remote Sensing, St. John's, Newfoundland, 12-13 August 1984.

Mobil Oil Canada. 1983. Grand Banks Operators Ice Management Plan.

Nathanson, F.E. 1969. Radar design principles. McGraw-Hill, New York.

North, D.O. 1963. An analysis of the factors which determine signal/noise discrimination in pulse carrier systems. Proceedings IEEE, July 1963.

Ryan, J.P. 1985. Enhancement of the radar detectability of icebergs 1986. Environmental Studies Revolving Funds, Report 022. Ottawa. 83 p.

Ryan, J.P. 1985. M.J. Harvey, and A. Kent. 1985. Assessment of marine radars for the detection of ice and icebergs. Environmental Studies Revolving Funds Report 008. Ottawa 127 p.

Sittrop, M. 1977. On the sea-clutter dependency on wind speed. Radar-77, International Conference, London, England, 25-28 October 1977.

Skolnik, M.I. 1970. Radar handbook. McGraw Hill, New York.

APPENDIX 1

ICEBERG CLASSIFICATION

APPENDIX 1

ICEBERG CLASSIFICATION

The icebergs were classified in size using the WMO/AES classification which is presented here.

Growler:

- height less than 1 m
- area usually about 20 m^2

Bergy Bit:

- height 1-5 m
- area usually 100-300 m^2

Icebergs:

a) all types except tabular

small
- height 5-15 m
- length less than 60 m

medium
- height 15-45 m
- length 60-120 m

large
- height 45-75 m
- length 120-210 m

very large
- height greater than 75 m
- length greater than 210 m

b) tabular icebergs

small
- height less than 6 m
- length less than 90 m

medium
- height 6-15 m
- length 90-120 m

large
- height greater than 15 m
- length greater than 120 m

Sizes refer to above-water portion only. If the length and height fell into different categories, the smaller class was assigned.

The shape description used is summarized as follows:

Tabular:

- iceberg having a very flat or horizontal top and near-vertical sides, greater length/height ratio than other icebergs.

Blocky:

- massive iceberg usually having steep precipitous sides and angular features, may have horizontal or flat top.

Dome:

- iceberg having large smooth rounded top, very solid iceberg.

Pinnacle:

- iceberg with large central spire or pyramid of one or more spies dominating shape; less massive than a dome iceberg of similar dimensions.

Dry Dock:

- iceberg having a flat sloping top and near vertical sides, one side higher than the other. The length/height ratio is usually higher.

The code (for example Berg 001 or Growler 003) associated with each iceberg are the designations given by Viatec when inputting ground truthing information and iceberg characteristics on the magnetic tape header.

APPENDIX 2

CALIBRATION RESULTS

APPENDIX 2

Throughout the program the power levels transmitted for each signal type were recorded approximately once a day. This was accomplished with a directional coupler which remained in the system to allow easy access to the power readings using the peak power meter and sensor. The configuration for recording of the power levels is shown in Figure 2.4 in the main text while Viatec Resource Systems Inc. retains a detailed set of calibration data. Averaging the readings produced Table A2-1.

Table A2-1.

Peak Power Readings Averaged

Description	X-Band (kilowatts)	S-Band (kilowatts)
Long Pulse	17.1	30.8
Medium Pulse	16.2	28.3
Short Pulse	7.5	14.3

It was noted that the S-Band readings were steady while the X-Band readings were fluctuating $\pm$ 0.4 kilowatts.

A reflection test was performed on both the X-Band and S-Band antennas. To accomplish this test the directional couplers were reversed and the power reflected back from the antenna systems was recorded. This amounted to a maximum of 6.5% of the output power transmitted from the transceiver was reflected back. This corresponds to 11.8 dB return loss or 0.29 dB transmission loss, which is about as expected.